

Adaptable Crosslinks in Polymeric Materials: Resolving the Intersection of Thermoplastics and Thermosets

Georg M. Scheutz,[‡] Jacob J. Lessard,[‡] Michael B. Sims, and Brent S. Sumerlin*[¶]

George & Josephine Butler Polymer Research Laboratory, Center for Macromolecular Science & Engineering, Department of Chemistry, University of Florida, Gainesville, Florida 32611, United States

ABSTRACT: The classical division of polymeric materials into thermoplastics and thermosets based on covalent network structure often implies that these categories are distinct and irreconcilable. Yet, the past two decades have seen extensive development of materials that bridge this gap through incorporation of dynamic crosslinks, enabling them to behave as both robust networks and moldable plastics. Although their potential utility is significant, the growth of covalent adaptable networks (CANs) has obscured the line between “thermoplastic” and “thermoset” and erected a conceptual barrier to the growing number of new researchers entering this discipline. This Perspective aims to both outline the fundamental theory of CANs and provide a critical assessment of their current status. We emphasize throughout that the unique properties of CANs emerge from the network chemistry, and particularly highlight the role that the crosslink exchange mechanism (i.e., dissociative exchange or associative exchange) plays in the resultant material properties under processing conditions. Predominant focus will be on thermally induced dynamic behavior, as the majority of presently employed exchange chemistries rely on thermal stimulus, and it is simple to apply to bulk materials. Lastly, this Perspective aims to identify current issues and address possible solutions for better fundamental understanding within this field.

1. INTRODUCTION

The year 2020 will mark the 100th anniversary of Hermann Staudinger's revolutionary macromolecular hypothesis, which first postulated the extended covalent structure of polymers and radically reshaped their chemical understanding.¹ From this foundation, nearly a century of research has led to a profound understanding of how macroscopic properties of polymeric materials emerge from molecular structure, and how this structure can in turn be manipulated to achieve efficient polymer production, processing, and performance.^{2,3} There is perhaps no clearer example of how structure affects function than in the comparison of thermoplastics, which contain unlinked polymer chains that may freely reptate throughout the material, with thermosets, in which covalent crosslinks bind the polymeric matrix into a single molecular unit. Consequently, thermoplastics can often be readily melted, deformed, and processed in the molten state,⁴ whereas thermosets feature exceptional thermal, chemical, and dimensional stability due to their permanent network structure. Yet this fixity comes at a price—thermosets are virtually

unrecyclable except through use as filler materials or decomposition through specialized chemical approaches.⁵ Considering the explosive growth of plastics waste resulting from difficulties in addressing end-of-life usage of polymeric materials,^{6,7} there is a pressing need for a new generation of materials that can be reprocessed like thermoplastics yet still retain the beneficial properties of a crosslinked thermoset material. Such a material could have scarcely been realized by historical polymer chemistry, but the emergence of covalent adaptable networks (CANs) over the past two decades has both highlighted the power of modern polymer chemistry while also challenging the traditional understanding of thermoplastics and thermosets.

Generally, adaptable networks are materials with crosslinks that are dynamic under specific stimuli, enabling recyclability⁸ while still retaining many of the beneficial properties of thermosets.^{9,10} These dynamic crosslinks can be either covalent bonds that undergo exchange with one another (i.e., CANs), or they can also consist of non-covalent interactions such as hydrogen bonding, host–guest interactions, or metal–ligand coordination (i.e., supramolecular adaptable networks).^{11–14} While we do not wish to underestimate the utility or elegance of materials crosslinked with supramolecular bonds¹⁵ (especially considering Nature utilizes many of these interactions to assemble exquisitely complex biomacromolecules), our discussions in this Perspective will focus on CANs as this crosslinking approach provides an exceptional combination of high mechanical performance, good recyclability, and facile implementation into applications.

Since the landmark report by Wudl in 2001 on heat-healable networks crosslinked with Diels–Alder adducts,¹⁶ numerous other reversible reactions and polymerization methods have been employed for CAN synthesis, and they are summarized in several of the excellent reviews on this subject.^{17–19} Bond exchange typically proceeds by one of two mechanisms: either a “dissociative” process in which crosslinks are cleaved into their individual constituent reactive partners before regenerating, or an “associative” process in which a pendent reactive group within the network undergoes a substitution reaction with an existing crosslink (Figure 1). This latter, associative process is characteristic of the recently developed and highly exciting “vitrimer” materials,²⁰ which exhibit properties that are beneficial for many high-performance applications. Yet, the rapid pace of recent developments has obscured the previously distinct line between thermoplastics and thermosets, and there have also emerged challenges and misconceptions in

Received: July 24, 2019

Published: September 16, 2019

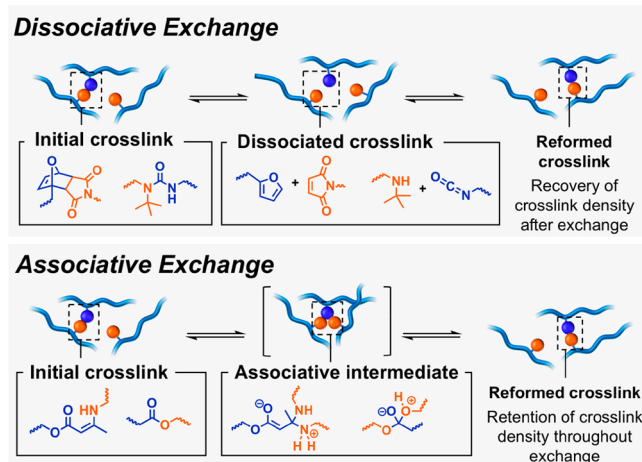


Figure 1. Depiction of dissociative and associative bond exchange pathways for covalent adaptable networks (CANs).

distinguishing dissociative and associative mechanisms of bond exchange in CANs. Our objectives in this Perspective are therefore to highlight the most enticing methods of accessing CANs while also summarizing the fundamental properties and behavior of these materials. We hope that in doing so, we will provide both new and experienced researchers in the field with a thorough sense of the state of the art as well as an unambiguous understanding of the characteristics of each class of CAN.

2. DISSOCIATIVE CANs

Overview. Dissociative CANs are crosslinked with reversible covalent bonds that, under a stimulus such as light or heat, enter into an equilibrium between open (dissociated) and closed (associated) states. Bond-breaking events lead to crosslink cleavage, and the network segments bearing the released reactive moieties can then diffuse through the network. After eventually encountering a complementary reactive moiety, the network segments can react and regenerate a crosslink. This repetitive process of dissociation, diffusion, and association, when occurring across an entire material, enables constructive deformation of otherwise unprocessable crosslinked materials. However, the necessity of initial crosslink dissociation imposed by the dissociative exchange mechanism introduces some practical challenges when working with dissociative CANs. As the instantaneous crosslink density of the CAN depends on the value of the equilibrium constant between associated and dissociated crosslinks (vide infra), the material properties can be quite sensitive to changes in stimulus and therefore less predictable than associative CANs. Additionally, full recovery of the original network integrity—together with the mechanical properties of the material—after removal of the stimulus requires all dissociated crosslinks to eventually react and reassociate. In reality, chain rearrangement, vitrification, or crosslink degradation can impede full crosslink reformation;¹⁷ therefore, dissociative CANs often exhibit different crosslink densities after processing.

Temperature is perhaps the simplest and most universal stimulus for modifying chemical processes, so it is unsurprising that thermoreversible networks are the most common type of dissociative covalent adaptable materials. Numerous thermor-

Dissociative Exchange of Dynamic Crosslinks

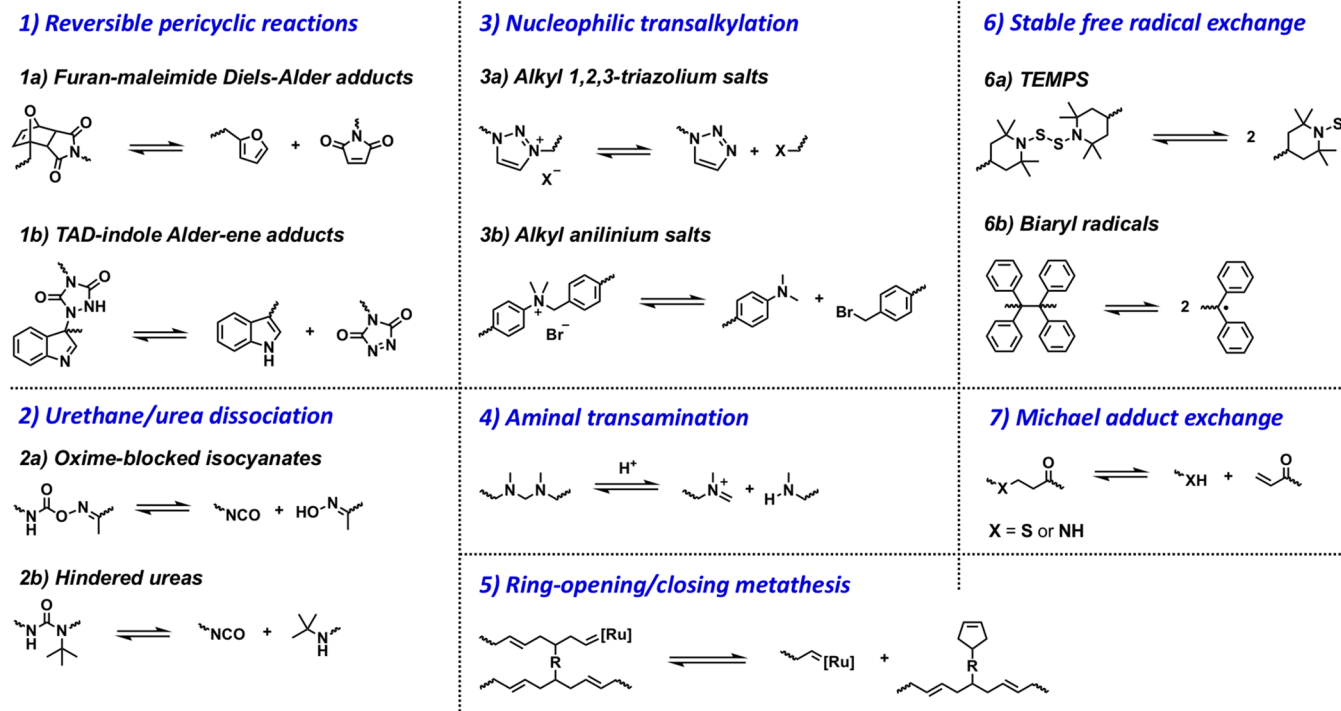


Figure 2. Overview of crosslinking chemistries utilized for dissociative covalent adaptable networks. See refs 23 and 24 (1a), 25 and 26 (1b), 30 (2a), 27–29 (2b), 31 and 32 (3a), 33 (3b), 35 (4), 40 (5), 43 and 44 (6a), 45 (6b), and 36 and 37 (7).

versible crosslinking chemistries for healable and reprocessable materials have been explored such as Diels–Alder (DA) cycloadditions,^{16,21–24} triazolinedione Alder–ene reactions,^{25,26} hindered urea exchange,^{27–29} oxime-enabled transcarbamoylation,³⁰ 1,2,3-triazolium^{31,32} and anilinium³³ transalkylation, boronate ester³⁴ and aminal bond³⁵ exchange, thiol–Michael³⁶ and aza-Michael³⁷ reactions, radical oligosulfide exchange,^{38,39} ring-opening metathesis polymerization (ROMP),⁴⁰ and persistent radical approaches using nitroxide,^{41,42} thionitroxide,^{43,44} or biaryl radicals.^{45,46} (Figure 2). Although photoreversible systems are beyond the scope of this Perspective, it is also worth noting that a remarkable degree of spatiotemporal control over bond exchange has been achieved in these types of dissociative CANs.^{9,47,48} In the following sections, we will explore many of these dynamic chemistries to illustrate the fundamental interrelationship between the association–dissociation equilibrium, gelation behavior of CANs, and ultimately the emergent material properties.

Dynamic Equilibrium between Associated and Dissociated Crosslinks. Two fundamental attributes of dissociative CANs profoundly impact their temperature-dependent viscoelastic behavior: the dynamic equilibrium of dissociative bond exchange, and the gel-point in association with the gel-point temperature. In thermoreversible dissociative CANs, the equilibrium between dissociated (open) and associated (closed) crosslinks—and thus the crosslinking density—is a function of temperature. For exothermic reactions ($\Delta H < 0$), increasing temperatures shift the equilibrium toward the reactants, thus lowering the crosslink density of the network and facilitating diffusion of network strands (Figure 3A).¹⁸ At high enough temperatures, when the equilibrium highly favors crosslink dissociation, the material

depolymerizes to a fluid (either a monomeric mixture or polymeric melt depending on the network composition), and upon cooling, it reverts back to a solid in a sol-to-gel transition when the reformation of crosslinks is favored.¹⁷ This was illustrated by work from Bowman and co-workers, who investigated the interdependence of temperature, chemical equilibrium, and the mechanical properties of networks crosslinked with furan-maleimide DA adducts (Figure 3B).²⁴ Upon heating, the mechanical properties of the material followed the trend expected for a thermoreversible network: at lower temperatures, the material behaved like a solid, whereas further heating of the sample led to a continuous decrease of the material's dynamic modulus until liquefaction occurred due to the shift of the chemical equilibrium toward dissociated DA crosslinks. In accordance with the observed viscoelastic behavior, K_{eq} decreased 13-fold from 10.7 to 0.8 M⁻¹ upon increasing the temperature from 45 to 112 °C, indicating a significant shift of the equilibrium toward crosslink dissociation (Figure 3C).

This unique dependence of crosslink density on a thermodynamic equilibrium imbues thermoreversible dissociative CANs with highly tunable, temperature-controlled mechanical properties. For instance, Pei and co-workers prepared DA crosslinked poly(acrylate) elastomers with tunable moduli by subjecting fully cured networks to temperatures between 90 and 160 °C to induce partial DA crosslink dissociation, followed by rapid cooling to room temperature, which prevented the complete reformation of the crosslinks.⁴⁹ Depending on the heating temperature, the moduli of the temperature-treated elastomers could be adjusted from 35 to 85% of the material's original elastic modulus. The lowest modulus was found in the network heated at the highest temperature (correlating to a high extent of crosslink dissociation), whereas lower heating temperatures (lower extent of crosslink dissociation) led to higher moduli. However, since DA association is thermodynamically favored at room temperature, an increase in the crosslink density and modulus of the temperature-treated elastomers over time could be observed.

It is important to note that at constant temperature, the crosslink density of thermoreversible CANs remains constant (Figure 3A). However, even at low temperatures where crosslink association is favored, dynamic bond exchange is still operative and can imbue networks with viscoelastic properties. For example, Xie and co-workers exploited the dynamic character of a furan–maleimide DA network to create remoldable shape-memory materials with solid state plasticity.⁵⁰ Linear bisphenol A-based polymers with furan side chains were crosslinked with a sub-stoichiometric amount of bismaleimide to obtain a DA network with a glass transition temperature of 35 °C. Even at temperatures as low as 60 °C, where the chemical equilibrium heavily resides on the side of the associated DA adducts, there was still sufficient bond exchange to dissipate applied stress, allowing the networks to exhibit complete stress relaxation. Exploiting this dynamic behavior, the crosslinked networks exhibited not only elastic shape adaptability (above T_g) and remoldability (after the gel-to-sol transition) but also plasticity in the solid state (at intermediate temperatures around 100 °C) for permanent shape reconfigurations. In the most extreme cases, DA networks can be fully depolymerized at high temperatures to recover the initial (macro)monomers, introducing a convenient mechanism for material reuse and recycling.⁵¹ In fact,

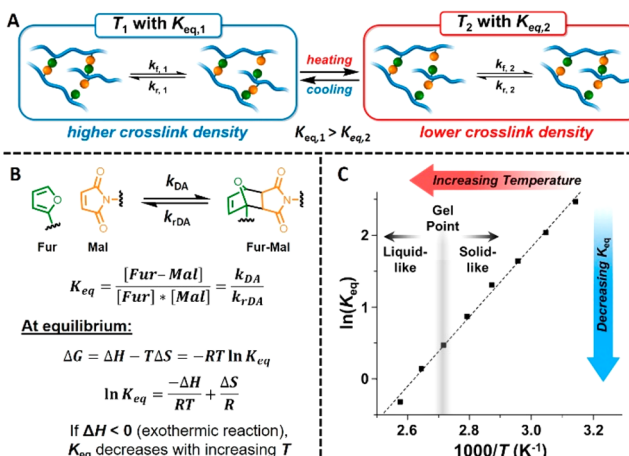


Figure 3. Relationship between temperature, chemical equilibrium, and material properties in thermoreversible dissociative CANs. (A) Thermoreversible dissociative CANs undergo dynamic bond exchange dictated by the rate constants for the forward and reverse reaction (k_f and k_r , respectively), corresponding to an equilibrium constant between open and closed crosslinks, K_{eq} . (B) Evaluation of equilibrium thermodynamics shows that, for an exothermic ($\Delta H < 0$) crosslink association process like the exchange of furan-maleimide Diels–Alder adducts, crosslink concentration decreases with increasing temperatures (see ref 18). (C) The van't Hoff plot obtained from a Fur-Mal crosslinked network shows a 13-fold decrease of K_{eq} upon increasing the temperature from 45 to 112 °C along with a gel-to-sol transition at 93 °C. Adapted with permission from ref 24. Copyright 2008 American Chemical Society.

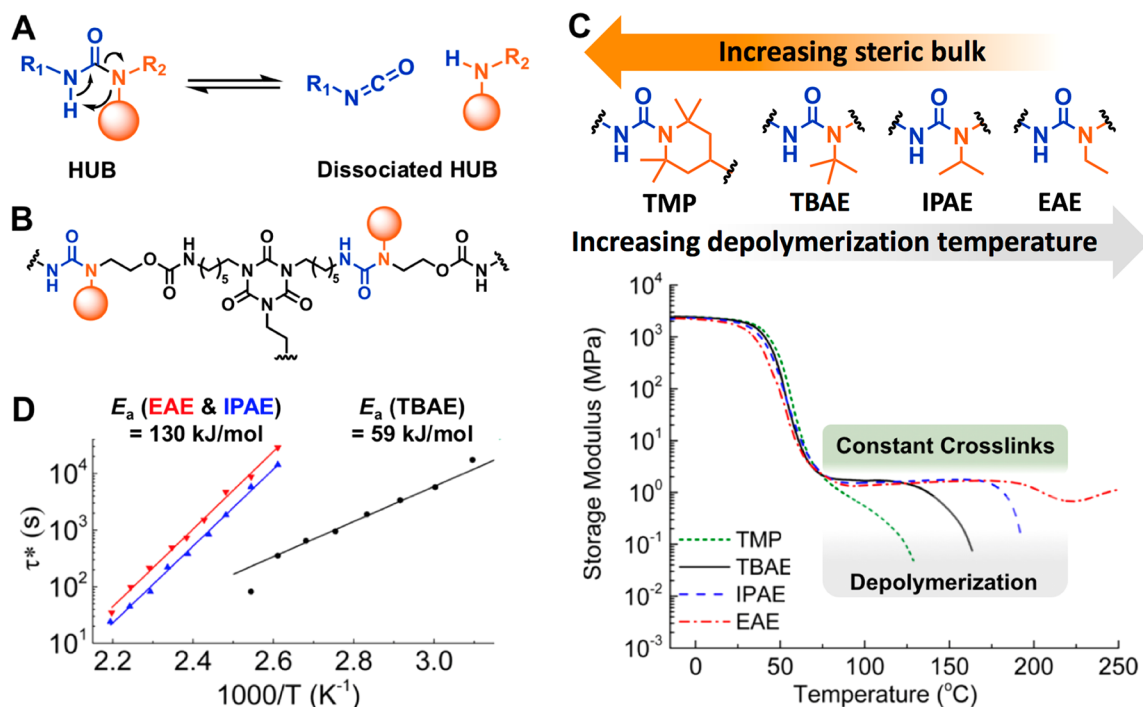


Figure 4. Effect of *N*-substituent sterics on the properties of hindered urea bond (HUB)-crosslinked networks. (A) Dissociative exchange of HUBs. (B) Schematic illustration of the chemical structure of the HUB network investigated by Rowan et al.²⁹ (C) Chemical structures of the HUB crosslinks displayed in order of their steric bulk (top). Dynamic mechanical analysis of the different networks shows constant rubbery plateaus for HUBs with lower steric hindrance (bottom). (D) The Arrhenius plot of the characteristic relaxation time τ^* versus inverse temperature shows a linearity within the boundaries of constant network integrity. Adapted with permission from ref 29. Copyright 2017 American Chemical Society.

recyclable DA-crosslinked materials based on industrially relevant polymers such as polyketones⁵² or ethylene-propylene rubbers⁵³ have been realized.

Gel-Point and Gel-Point Temperature. For irreversibly crosslinked materials, the gel-point describes the well-defined stage of a polymerization at which an infinite network arises. Mathematically, this can be defined as the reactive group conversion where the weight-average molecular weight diverges.^{54,55} CANs are no different, but the thermoreversible nature of crosslinking also introduces a temperature dependence of crosslink conversion. Therefore, a new parameter describing the gel-point needs to be considered: the gel-point temperature (T_{gel}).¹⁸ Critically, once the crosslink exchange process reaches equilibrium, the crosslink density is time-independent but can be modified by changing the temperature. This feature was leveraged by Bowman and co-workers to conveniently and accurately measure the viscoelastic properties of a network linked by furan-maleimide adducts near the gel-point.²⁴ Using the Winter-Chambon criterion for gelation (i.e., $\tan \delta$ is frequency-independent at the gel-point) to precisely find the gel-point temperature of the network, the authors found that the equilibrium conversion of DA adducts at T_{gel} ($70.9 \pm 0.5\%$) was in excellent agreement with the theoretical gel-point as predicted by Flory-Stockmayer theory (70.7%). The consistency between theory and experiment is particularly appealing, because the prediction of the viscoelastic properties of dissociative CANs requires the assessment of the crosslink conversion relative to the Flory-Stockmayer gel-point.

Mathematically, this can be rationalized through the Semenov-Rubinstein (SR) model of thermoreversible gelation.⁵⁶ Treating thermoreversible networks as clusters comprising multiple joined polymer chains with reversible crosslinks as

junction points, SR theory shows that the viscoelastic response of a thermoreversible network can be predicted by taking into account the time scale of deformation, the effective lifetime of the reversible crosslink, and the crosslink conversion with respect to the Flory-Stockmayer gel point. At crosslink conversions well below the gel-point ($T \gg T_{\text{gel}}$), the presence of dynamic crosslinks has little effect on the material response, and the viscoelastic properties are dominated by unreacted (macro)monomers. Close to the gel-point ($T \approx T_{\text{gel}}$), the longest conformational relaxation time increases as more and more chains associate in larger clusters, and depending on the average crosslink lifetime, these clusters break into a set of smaller sub-clusters with shorter relaxation times. Above the gel-point ($T \ll T_{\text{gel}}$), when the cluster size is above the percolation threshold, full relaxation of the network can only occur via reversible crosslink dissociation. In this regime, the terminal relaxation time scales with the crosslink lifetime and the distance from the Flory-Stockmayer gel-point in terms of conversion. However, it should be noted that, in this regime, the effective lifetime of a dynamic bond is much longer than the time scale of individual association/dissociation events. Conformational changes (and therefore network relaxation) through dynamic bond cleavage require a released reactive group to find a *different* partner, yet the instantaneous concentration of free reactive groups is very low above the gel-point ($T \ll T_{\text{gel}}$). Therefore, in the example of a network crosslinked with furan-maleimide adducts, a particular adduct may dissociate and reassociate many times before its furan or maleimide constituents will be able to find a different reaction partner. This phenomenon also leads to an activation energy (E_a) of viscous flow that is higher than the E_a of the bond exchange itself.⁵⁷ Agreement between the SR model and the viscoelastic behavior of DA networks above the gel-point was

proven in a seminal study by Sheridan et al.⁵⁸ and later by Wang and co-workers.⁵⁹ Although more dissociative CAN chemistries need to be analyzed, the applicability of the SR model (and potentially modifications thereof)^{60,61} to this type of material with strong reversible covalent crosslinks could pave the way for better understanding and description of the rheological behavior of dissociative CANs.

Vitrimer-Like Thermoreversible Dissociative CANs. The crosslink density in thermoreversible dissociative CANs inevitably decreases with increasing temperature, as dictated by the temperature-dependent dynamic equilibrium (Figure 3B). However, isochronal dynamic mechanical analysis of various thermoreversible dissociative CAN systems (e.g., hindered urea,²⁹ 1,2,3-triazolium,^{31,32} nitroxide,⁴² DA,^{59,62} acetoacetyl amide,⁶³ or oxime-carbamate³⁰ networks) revealed a rubbery plateau of constant modulus between the glass transition and the gel point (Figures 4, 5, and 6). This suggests that, since the

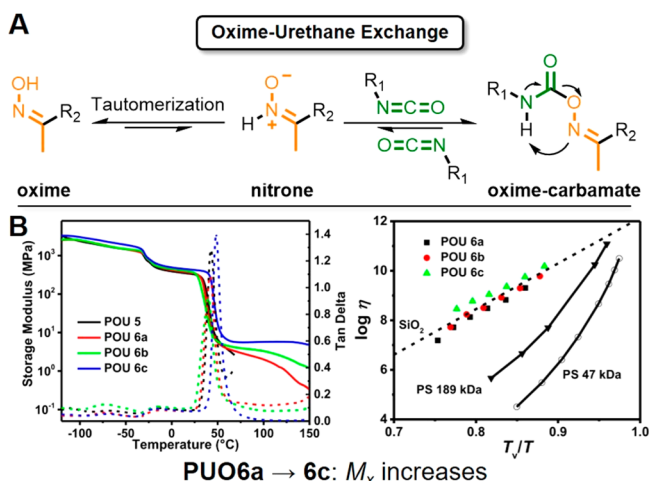


Figure 5. Exchange mechanism and mechanical properties of oxime-blocked isocyanate networks. (A) Proposed mechanism for the dissociative transcarbamoylation of oxime-carbamates. (B) Dynamic mechanical analysis (left) of linear oxime carbamate polymers (POU 5) and networks (POU 6a–6c) showing a glass transition of the glassy oxime-carbamate block followed by a constant rubbery plateau for the networks dependent on their crosslink density (M_x). The Angell fragility plot (right) of PUO 6a–6c indicates a gradual decrease of viscosity with temperature similar to silica. Reproduced with permission from ref 30. Copyright 2017 American Chemical Society.

modulus at the rubbery plateau can be related to the network's crosslink density, K_{eq} at these temperatures is large and strongly favors crosslink association. Therefore, the absolute variability of crosslink density within this temperature range appears to be too small to significantly impair the overall network integrity, causing dissociative CANs to behave similarly to vitrimers in this temperature region, as will be shown in upcoming examples.

This vitrimer-like behavior is clearly shown through work by Rowan and co-workers on the behavior of dissociative poly(urethane-urea) networks containing hindered urea bonds (HUBs) (Figure 4).²⁹ Unlike typical urea linkages, HUBs contain a bulky *N*-substituent that distorts the conjugation between the nitrogen and the carbonyl orbitals, thus facilitating thermoreversible dissociation into isocyanate and amine components (Figure 4A).^{27,28} A series of poly(urethane-urea) networks was generated by reacting a

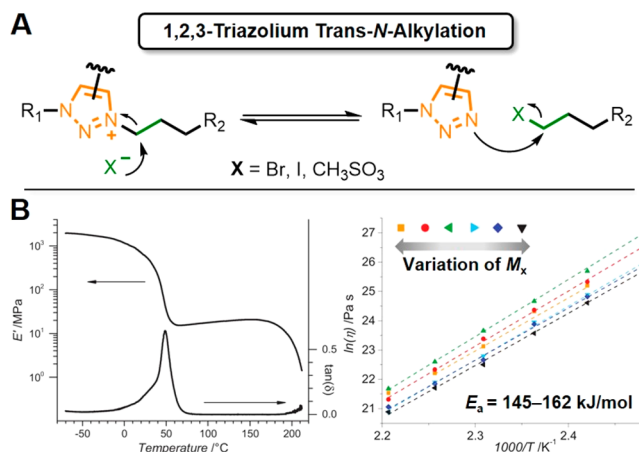


Figure 6. Exchange mechanism and mechanical properties of 1,2,3-triazolium networks. (A) Proposed mechanism of counterion-mediated dissociation of 1,2,3-triazolium crosslinks. (B) Dynamic mechanical analysis (left) of a 1,2,3-triazolium iodide network shows a constant rubbery plateau spanning from 50 to 175 °C. The linear Arrhenius plot shows similar values for the energy of activation (E_a) of viscous flow for 1,2,3-triazolium iodide networks with different crosslink densities (M_x). Adapted with permission from ref 32. Copyright 2017 Wiley.

triisocyanate with four different amino alcohols bearing increasingly bulky ethyl (EAE), isopropyl (IPA), *tert*-butyl (TBAE), and 2,2,6,6-tetramethylpiperidine (TMP) groups as *N*-substituents (Figure 4B,C).²⁹ The onset temperature of network dissociation, seen as a sharp decrease in modulus upon heating, exhibited a clear dependence on substituent bulk, with decreasing network dissociation temperatures observed for increasingly bulky HUBs (Figure 4C). While TMP-containing networks began to flow immediately after the glass transition, the less sterically encumbered EAE-, IPA-, and TBAE-containing networks exhibited distinct rubbery plateaus, suggesting that the K_{eq} value for these materials remains high until the dissociation temperature is reached. This was confirmed through variable-temperature Fourier transform-infrared (FT-IR) spectroscopy, which indicated that the dissociation of EAE and IPA HUBs remained below 1% up to 170 °C, while the dissociation of TBAE reached ~8% at 130 °C. Importantly, similar behavior has also been observed for other CAN chemistries and topologies, such as chain-growth networks with reversible crosslinks pendent to the backbone^{42,59,62} and pure step-growth materials.^{29–32} Finally, stress relaxation of TBAE, EAE, and IPA networks in the range of their rubbery plateau scaled according to an Arrhenius relationship, with lower E_a values calculated for bulkier HUB substituents (Figure 4D).

Although also observed in thermoplastic polymer melts well above T_g ($\sim T_g + 100$ °C),^{64,65} the Arrhenius dependence of viscosity on temperature is usually ascribed to associative CANs, and is commonly considered as a hallmark property unique to associative exchange. However, like the hindered urea networks, many thermoreversible dissociative CANs also exhibit an Arrhenius temperature dependence of viscosity and stress relaxation at temperatures below T_{gel} , where K_{eq} and crosslink conversion are high.^{26,29–32,35,45,48,59,62,63} In accordance with the SR theory (vide supra), this suggests that within a certain temperature range below T_{gel} , where network integrity is maintained with a sufficient crosslink density, that stress relaxation is governed by bond exchange, and therefore

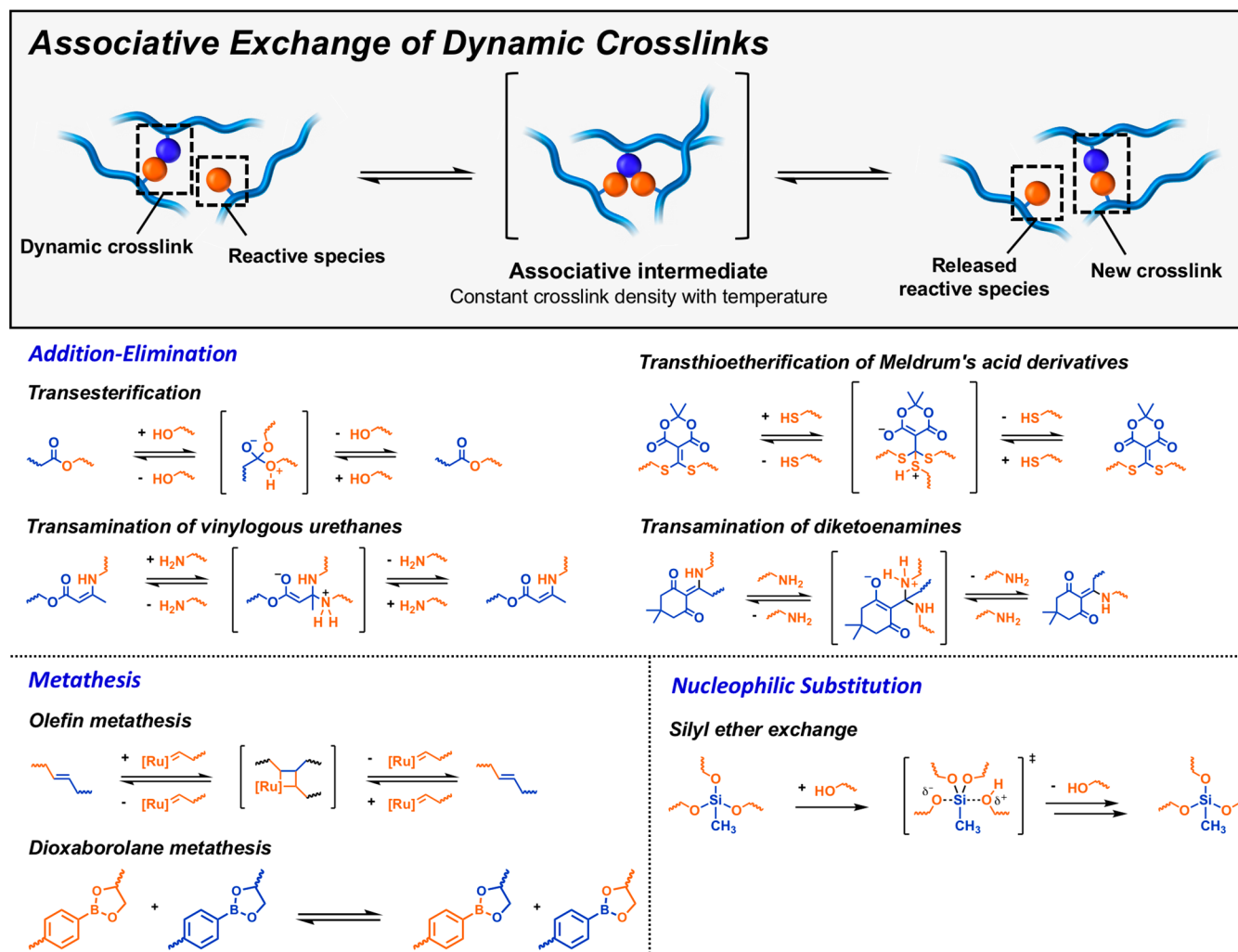


Figure 7. General mechanism of associative bond exchange and overview of crosslinking chemistries utilized for associative covalent adaptable networks. See refs 66–68 (transesterification), 69–71 (vinyllogous urethanes), 72 (thiol exchange), 76 (diketoenamines), 77 (olefin metathesis), 78 (dioxaborolanes), and 74 and 75 (silyl ethers).

dissociative CANs can exhibit properties resembling associative CANs. For example, Liu et al. generated highly dynamic polyurethane derivatives by employing thermoreversible oxime-blocked isocyanate crosslinks (Figure 5).³⁰ DMA analysis showed a rubbery plateau for all oxime-carbamate networks after the glass transition around 30 °C. Notably, the network with the highest crosslinking density (PUO 6c) maintained its network integrity over the widest temperature range. Viscosity was obtained from stress relaxation experiments using the Maxwell relation and was found to gradually decrease with temperature according to the Arrhenius law. Molecular modeling of the oxime-enabled transcarbamoylation reaction supported a dissociative pathway (Figure 5A), which was further corroborated by the complete dissolution of the networks at 110 °C in *N,N*-dimethylacetamide. Notably, the slightly basic oxime nitrogen in the β -position to the carbonyl could facilitate an intramolecular proton abstraction from the amide nitrogen in the first step of the exchange reaction, suggested as the reason for the rapid bond exchange of oxime-carbamates at moderate temperatures in comparison to conventional urethanes. In fact, a similar reaction sequence (tautomerization followed by intramolecular proton transfer) is

also believed to endow vitrimer-like dissociative acetoacetyl amide networks with remarkably fast exchange kinetics.⁶³

Assessment of the bond exchange kinetics in combination with rheological analysis is pivotal for a full description of the properties of thermoreversible dissociative CANs. Using an innovative combination of X-ray photoelectron spectroscopy (XPS) and rheology, Obadia et al. were able to elucidate the exchange mechanism of 1,2,3-triazolium crosslinked ionic networks.³² As described in an earlier report from the same group, CANs were accessed via a Huisgen 1,3-dipolar cycloaddition of linear α -azido- ω -alkyne monomers followed by in situ crosslinking of the resultant internal 1,2,3-triazoles with alkyl dihalides or dimesylates.³¹ While an associative mechanism for bond exchange could be imagined via a concerted $S_{N}2$ transalkylation between free 1,2,3-triazoles and *N*-alkylated 1,2,3-triazolium junction points, it was instead shown that bond exchange proceeded through initial dealkylation of the 1,2,3-triazolium crosslink by the halide counterion (dissociation) followed by attack on the newly formed alkyl halide by a different 1,2,3-triazole (association, Figure 6A). Using 1,2,3-triazolium networks with varying crosslink densities, a correlation of the characteristic relaxation time (obtained from stress relaxation experiments) with the

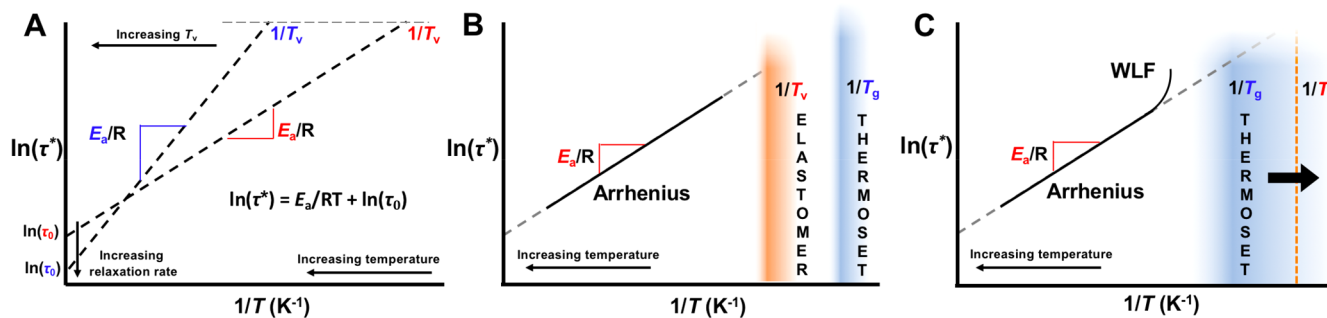


Figure 8. Schematic Arrhenius plots for systems with a different activation energy (E_a) and Arrhenius prefactor (τ_0), as well as the effect of the glass transition temperature (T_g) and topology freezing temperature (T_v). (A) E_a as the slope of the Arrhenius fit is a measure for the temperature sensitivity of viscosity. A larger E_a (i.e., a higher slope, shown in blue) indicates more rapid changes of viscosity with temperature. The y -intercept of the Arrhenius fit marks τ_0 , which can be interpreted as the relaxation time without thermal constraints. (B) Hypothetical Arrhenius plot for a system with $T_v > T_g$. (C) Hypothetical Arrhenius plot for a system with $T_v < T_g$. After traversing T_g the viscosity follows a Williams–Landel–Ferry (WLF) model before entering an Arrhenius fit.

total concentration of alkyl iodide moieties (determined by XPS) was discovered, which corroborates with the dissociative exchange mechanism.³² In a similar example, a dissociative mechanism involving a counterion-mediated transalkylation of quaternary nitrogen compounds was also suggested by Konkolewicz and co-workers, using dynamic networks cross-linked by quaternary anilinium compounds.³³ The 1,2,3-triazolium-crosslinked networks exhibited a constant rubbery plateau over a long temperature range before depolymerization (~ 175 °C) and Arrhenius temperature dependency of viscosity (Figure 6B), which evokes the properties exhibited by vitrimeric materials. This stands in sharp contrast to the common assertion that vitrimeric and dissociative CANs exhibit clearly distinct viscoelastic properties. We therefore argue that the conventional method of proving vitrimeric behavior—the observation of Arrhenius stress relaxation—is insufficient and should be accompanied by further evidence of an associative crosslink exchange mechanism versus a dissociative mechanism.

3. ASSOCIATIVE CANs: “VITRIMERS”

Overview. Like their dissociative counterparts, associative CANs are crosslinked polymer materials with exchangeable covalent bonds that can enter into a dynamic equilibrium for crosslink exchange. However, bond-breaking and bond-forming in associative CANs occur in a single reaction rather than in discrete dissociation and association steps (Figure 7). As a result, these materials exhibit a viscosity–temperature relationship similar to that of vitreous silica, which inspired Leibler to coin the term “vitrimer” for these materials.^{20,66} The key advantage imparted by the associative exchange mechanism is the retention of crosslink density, even at very high temperatures or in the presence of solvent—conditions that would promote crosslink dissociation in dissociative CANs. Accordingly, significant effort has been devoted toward new methodologies for achieving associative exchange. To date, transesterification^{20,66–68} and transamination of vinyl-^{69–71} are perhaps the most developed chemistries for associative CANs, and new approaches relying on thiol exchange,⁷² transalkylation of trialkylsulfonium salts,⁷³ silyl ether transalkoxylation,^{74,75} diketoenamine exchange,⁷⁶ olefin metathesis,⁷⁷ and dioxaborolane metathesis⁷⁸ have also been suggested. In the upcoming discussion, we will outline the key rheological features of associative CANs followed by an

exploration of the chemistries that have been utilized for their synthesis.

Viscous Flow in Associative Networks: Arrhenius Relationship.

Unlike dissociative networks, crosslink exchange in associative networks is a degenerative process; that is, the chemical entities on both sides of the equilibrium are identical, and thus neither side of the reaction is favored with temperature. With no thermodynamic bias to either side of the reaction, K_{eq} remains constant with increasing temperature, and only the exchange rate is accelerated.¹⁸ Furthermore, because the constant crosslink density limits diffusion of network strands, it is often assumed that the rate of dynamic crosslink exchange dictates viscous flow. As a result, the gradual decrease of viscosity with increasing temperature for associative CANs can be modeled with an Arrhenius relationship. Since viscosity and the characteristic relaxation time τ^* are connected via the Maxwell relation, one can use stress relaxation experiments to examine the temperature dependence of viscosity by fitting τ^* to the general Arrhenius equation:

$$\tau^* = \tau_0 \exp\left(\frac{E_a}{RT}\right) \quad (1)$$

where τ_0 is the Arrhenius prefactor and E_a is the activation energy for viscous flow. However, it should be noted that this E_a can be markedly different from the E_a of an analogous small molecule exchange reaction, particularly in networks where crosslink exchange requires significant network strand reorganization (e.g., networks that contain a low fraction of exchangeable moieties).^{72,75,78} In addition to providing insight into the chemical and physical processes that lead to network reorganization, the E_a of viscous flow describes the sensitivity of the viscosity of associative CANs to temperature changes, which is also illustrated in the Arrhenius plot where E_a determines the slope of the curve (Figure 8A). High values for E_a indicate a fast decrease of viscosity upon increasing temperatures, whereas vitrimer with low E_a show less pronounced viscosity changes. This behavior could be conveniently utilized for the implementation of vitrimer materials into practical applications, in which systems with high E_a values should show improved dimensional stability at service temperatures due to the high energy barrier of bond

exchange, yet the rapid decrease of viscosity with increasing temperatures would enable fast processing on demand.³²

The Arrhenius prefactor (τ_0) is the extrapolation of the Arrhenius plot to infinite temperature and can be interpreted as the characteristic relaxation time if network rearrangement is barrierless (Figure 8A).⁶⁸ In general, a network with a lower τ_0 value will relax faster than a network with the same E_a for viscous flow but a higher τ_0 value. However, it is important to note that neither E_a nor τ_0 are absolute parameters by themselves. For a concise description of the flow properties of vitrimers, both E_a of viscous flow and τ_0 must be taken into consideration, and care should be taken when comparing vitrimers with different exchange chemistries and network topologies.

Viscous Flow in Associative Networks: Glass Transition and Topology Freezing Transition. Viscous flow in vitrimers requires both sufficient network strand mobility ($T > T_g$) as well as a sufficient rate of crosslink rearrangement to accommodate deformations. Although crosslink exchange theoretically occurs to some extent at all temperatures, an additional transition temperature, the topology freezing temperature (T_v), can be defined that relates to the temperature at which crosslink exchange becomes sufficiently rapid to enable network reorganization. This transition is typically observed as a transition from an elastic solid to a flowing viscoelastic material in situations where the network is not vitrified (i.e., above the T_g), and by convention, T_v is defined as the temperature at which the network reaches a viscosity of 10^{12} Pa·s.²⁰ Generally, one can imagine two different scenarios: When T_v is greater than T_g , the material is a glass below and an elastomer above T_g . Once the temperature is above T_v , the material's viscosity gradually decreases following the Arrhenius law (Figure 8B). In the second scenario, T_g is greater than the hypothetical T_v , so the material is a glass at all temperatures below T_g as bond exchange is suppressed due to the lack of chain mobility. As the temperature passes the T_g , the material briefly behaves according to the Williams–Landel–Ferry (WLF) model before following the Arrhenius dependence (Figure 8C).⁷⁵ Therefore, the start of flow for vitrimer materials is dictated by the highest transition temperature of the material (T_g or T_v).

Catalytically Activated Vitrimers. Having outlined the fundamental chemical and physical properties of vitrimers, we will now highlight several key advances in the field since its recent inception. The first practical vitrimer materials, reported by Leibler and co-workers in 2011, were epoxy-carboxylic acid networks, where bond exchange was enabled by the $Zn(acac)_2$ -catalyzed transesterification of ester linkages with free hydroxyl groups (Figure 9A),²⁰ a technique that has been widely used for the modification and processing of polyester and polycarbonate materials.^{79,80} Below the glass transition temperature (~ 80 °C), the material was found to behave as a glassy thermoset, yet at 200 °C it could be reversibly deformed. Furthermore, even after being ground into a powder, the network could be fully recovered after heating for only 3 min at 200 °C. The mechanism behind the high efficiency of crosslink exchange was later revealed by extended X-ray absorption fine-structure spectroscopy and FTIR studies, which showed that the zinc cation (Zn^{2+}) of the catalyst becomes tetracoordinated to the oxygen atoms of the β -hydroxyester moieties, simultaneously bringing the exchange partners in spatial proximity and activating the ester carbonyl bond.⁸¹

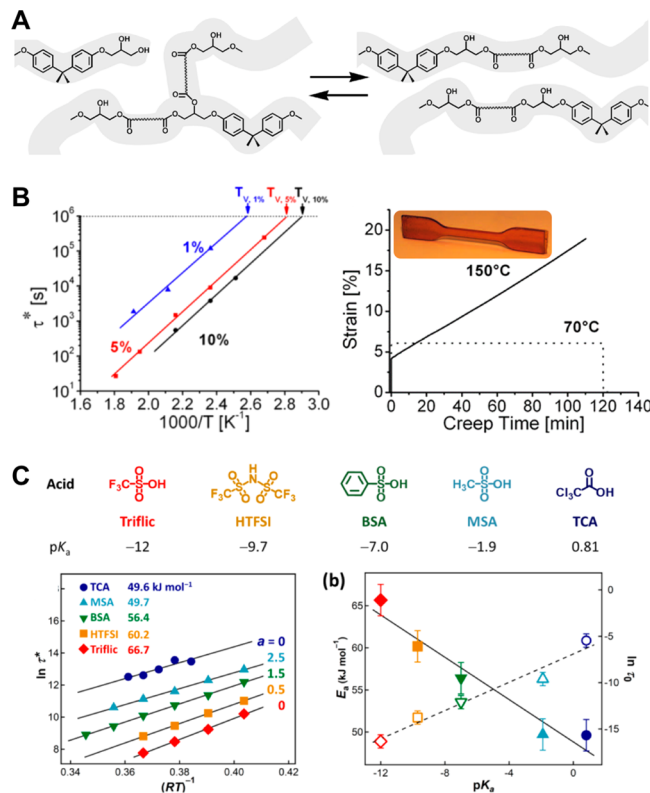


Figure 9. Influence of catalyst loading and catalyst identity on the viscoelastic properties of transesterification vitrimers. (A) Transesterification in β -hydroxyester epoxy networks. Reproduced with permission from ref 20. Copyright 2011 AAAS. (B) Arrhenius plot of the characteristic relaxation time (τ^*) obtained from stress relaxation experiments for 1 mol% (blue), 5 mol% (red), and 10 mol% (black) $Zn(OAc)_2$ (left), and elongational creep experiments at 70 °C (below T_v) and 150 °C (above T_v) (right). Reproduced with permission from ref 82. Copyright 2012 American Chemical Society (C) Transesterification of vitrimer networks under Brønsted-acid catalysis. Stress relaxation data depicts an Arrhenius dependence of τ^* on temperature for all five Brønsted acids (left), and both activation energy (E_a , filled symbols) and Arrhenius prefactor (τ_0 , open symbols) are strongly correlated with Brønsted acidity (pK_a). Reproduced with permission from ref 68. Copyright 2018 American Chemical Society.

It should be noted that the use of an external catalyst is not solely a synthetic necessity; in fact, manipulation of the catalyst can enable a remarkable degree of control over the viscoelastic behavior of the vitrimers. Leibler and co-workers demonstrated this property by incorporating 1, 5, and 10 mol% $Zn(OAc)_2$ catalyst into β -hydroxyester vitrimers and showing that increased catalyst loading corresponds to faster stress relaxation.⁸² Interestingly, Arrhenius fits of the stress relaxation data revealed that the E_a for viscous flow did not change with catalyst concentration, but instead a progressive decrease of τ_0 was observed (Figure 9B). This behavior implies that increasing the catalyst loading will improve the processability of the material at elevated temperatures due to faster stress relaxation arising from a short τ_0 , but the change in the rate of bond exchange as a function of temperature (governed by the E_a) will remain unaltered. Accordingly, T_v was found to increase with decreasing $Zn(OAc)_2$ content (Figure 9B)—an attractive feature for the generation of vitrimer materials with improved creep resistance, since excellent dimensional stability was observed in creep experiments with $Zn(OAc)_2$ -catalyzed transesterification catalysts at temperatures below T_v .⁸²

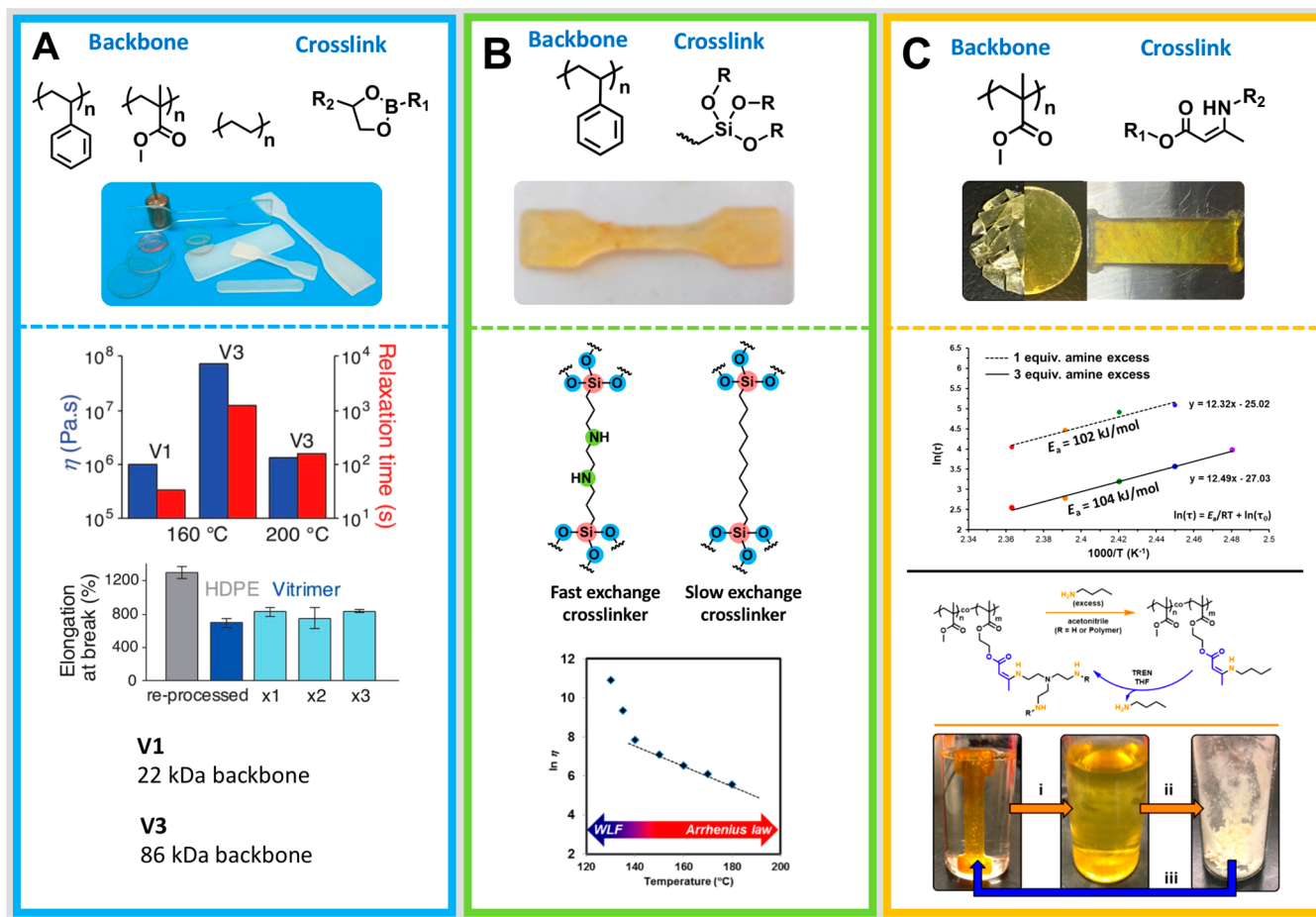


Figure 10. Vitrimeric polymer plastic mimetics from commodity plastics. (A) Chemical structures and mechanical properties of dioxaborolane PMMA, PS, and HDPE vitrimers. The viscosity and relaxation time for the dioxaborolane PMMA vitrimer increase significantly with increasing molecular weight (top). The elongation at break is reduced for the HDPE vitrimer compared to HDPE, but stays constant over three reprocessing cycles. Reproduced with permission from ref 78. Copyright 2017 AAAS. (B) Chemical structures and stress relaxation of silyl ether PS vitrimers. The Arrhenius plot of viscosity shows the change from Williams–Landel–Ferry (WLF) to Arrhenius behavior for silyl ether vitrimer networks. Reproduced with permission from ref 75. Copyright 2017 American Chemical Society. (C) Chemical structure and Arrhenius plot of vinyllogous urethane PMMA vitrimer with 1 and 3 equiv excess amine. Faster stress relaxation is observed at higher amine content. Reproduced with permission from ref 71. Copyright 2019 American Chemical Society.

An alternative approach to tuning the rate of bond exchange in vitrimers is to change the identity of the catalyst rather than simply varying its concentration. In the previously discussed work, Leibler and co-workers studied the effect on network stress relaxation of changing the catalyst from $\text{Zn}(\text{OAc})_2$ to either triazabicyclodecene (TBD) or triphenylphosphine ($\text{P}(\text{Ph})_3$). As would be anticipated, changing the catalyst alters the mechanism of bond exchange, and different values of E_a were measured for each different catalyst ($E_{a,\text{TBD}} > E_{a,\text{Zn}(\text{OAc})_2} > E_{a,\text{P}(\text{Ph})_3}$). Later, this effect was elegantly illustrated by Bates and co-workers, who used Brønsted acid catalysis to tune the mechanical properties of low- T_g polyester vitrimers and in fact discovered that the rate of bond exchange correlated with the pK_a of the acid catalyst (Figure 9C).⁶⁸ Stronger acids led to higher E_a values while providing faster stress relaxation at sufficiently high temperatures (shorter τ_0) than weaker acids. Similar results have also been reported in other transesterification vitrimers using zinc acetylacetone⁸³ or tin-based catalysts^{84,85} as well as in the realm of vinyllogous urethane vitrimers,⁷⁰ suggesting that rational catalyst design

can be a powerful tool to tune the viscoelasticity of vitrimeric materials.

Catalyst-Free Vitrimers. While the use of catalysts can enable associative bond exchange in otherwise inert linkages and control over viscoelastic properties of a given network, there are some situations in which the presence of a catalyst can be disadvantageous. Exogenous catalysts can degrade or leach over time, and it may also be desirable to incorporate structural units in a network that are incompatible with the employed catalyst. There has therefore been significant effort devoted toward developing new associative bond exchange reactions that are thermally activated under uncatalyzed conditions. In a seminal report, Du Prez and co-workers utilized transamination of vinyllogous urethanes at 100–140 °C for the preparation of catalyst-free vitrimers.⁶⁹ Similar to acyl substitution, associative exchange in vinyllogous urethane vitrimers proceeds through an addition–elimination mechanism that involves attack of a free primary amine on the vinyllogous urethane β -carbon, subsequently releasing a new primary amine (Figure 7). At elevated temperatures (130–170 °C) in the absence of catalyst, vitrimers containing these dynamic crosslinks exhibited complete stress relaxation, and

fragmented samples could be fully reprocessed into healed materials by compression molding within short time scales (30 min or less). While bond exchange in vinylogous urethane materials appreciably proceeds in the absence of catalyst, it was later shown by the same group that viscoelastic properties could be tuned by introducing a Brønsted base or Brønsted/Lewis acid additive.⁷⁰ Notably, the addition of the strong base TBD slowed down exchange significantly and even inhibited bond rearrangements at higher loadings, whereas acidic additives (e.g., *p*-toluenesulfonic acid and dibutyltin dilaurate), were shown to accelerate bond rearrangements.

The catalyst-free concept was further developed by Kalow and co-workers, who successfully adapted a recently developed reaction⁸⁶ involving the exchange of thiols via a conjugate addition–elimination reaction with an acceptor derived from Meldrum's acid for the synthesis of vitrimeric silicone elastomers (Figure 7).⁷² The use of a catalyst-free protocol was necessary in this case due to the sensitivity of Si–O bonds to acids and bases; nevertheless, the materials could be reprocessed over 10 total cycles with no observable change in thermal or mechanical properties. Intriguingly, these materials featured exceptionally low T_g ($-106\text{ }^\circ\text{C}$) and T_v ($-6\text{ }^\circ\text{C}$) values, which suggests the probability of creep at room temperature. However, these materials were observed to lack appreciable creep even under a constant 37 kPa stress at room temperature. The authors therefore concluded (a conclusion with which we concur) that this result may indicate that a simplistic view of the interplay between T_g and T_v might be insufficient to predict the properties of vitrimer materials.⁷²

Finally, we wish to emphasize that several other catalyst-free vitrimers have been developed in addition to the discussed approaches, such as materials that rely on the exchange of silyl ethers,^{74,75} vinylogous ureas,⁸⁷ dioxaborolanes,⁷⁸ boroxines,^{88,89} and hydroxyurethanes.⁹⁰ There is also a particular advantage to using systems that can operate with or without a catalyst. The use of a catalyst enables a wide range of tunable mechanical properties, yet the material still retains an inherent degree of bond exchange and reprocessability without a catalyst. This could allow the beneficial aspects of catalyzed associative bond exchange (e.g., rapid reprocessability) to be accessed while mitigating the potential deleterious impact of catalyst loss from the material over time.

Vitrimeric Mimetics of Commodity Materials. Arguably the critical bottlenecks in the translation of the vitrimer concept to everyday use are the availability of methodologies that source vitrimers from inexpensive chemical feedstocks and the development of vitrimeric materials with many properties analogous to those of the current commodity polymers. Nicolay, Leibler, and co-workers took the first steps in this direction by applying the vitrimer concept to commercially relevant polymers, such as high-density polyethylene (HDPE), polystyrene (PS), and PMMA (Figure 10A).⁷⁸ The exchangeable moieties implemented were dioxaborolanes that were proposed to undergo metathesis with each other to allow the material to flow, and straightforward protocols were developed to enable their incorporation in each polymer. HDPE vitrimers were observed to have similar mechanical strength ($E \approx 19\text{ MPa}$) but lower elongation at break ($\sim 800\%$) compared to the commodity materials ($\sim 1300\%$) due to the permanent network structure of the vitrimer (Figure 10A). Furthermore, the tensile strengths of the PS ($E \approx 1.4\text{ GPa}$) and PMMA ($E \approx 1.8\text{ GPa}$) vitrimers were similar to those of the thermoplastic commodity materials ($E_{\text{PMMA}} \approx 1.7\text{ GPa}$, $E_{\text{PS}} \approx 1.5\text{ GPa}$).

Finally, the mechanical properties of the vitrimer materials were maintained over four destruction–injection molding cycles. We emphasize that these vitrimers, by virtue of their crosslinked structure, would likely exhibit superior mechanical and solvent resistance compared to their uncrosslinked counterparts while still retaining similar physical properties. It was additionally shown that HDPE and PMMA vitrimers could be welded together as a result of dynamic bond exchange at the interface of the two materials, resulting in strong adhesion between the two polymers—an unattainable result with conventional thermoplastic materials.

Additional chemistries have since been employed for the synthesis of vitrimeric derivatives of commodity materials. The Guan group used the exchange of silyl ethers to develop vitrimeric PS mimetics by crosslinking pendent hydroxyl-functional PS ($M_n = 29.0\text{ kg/mol}$) with a sub-stoichiometric amount of silyl ether to form vitrimer networks (Figure 10B).⁷⁵ Associative bond exchange was enabled by the exchange of the resultant silyl ether crosslinks with residual free hydroxyl groups. It was additionally shown that by changing the identity of the silyl ether γ -substituent from a methylene group to a secondary amine, the rate of crosslink exchange could be accelerated through neighboring group participation (Figure 10B), evidenced by a decrease in E_a for viscous flow from 174 kJ mol^{-1} for methylene-containing vitrimers to 81 kJ mol^{-1} for amine-containing vitrimers. Remarkably, these latter materials also provided the first experimental verification of a vitrimer with a T_v ($47\text{ }^\circ\text{C}$) lower than its T_g ($125\text{ }^\circ\text{C}$), and the behavior predicted a year earlier by Denissen, Winne, and Du Prez¹⁹ was confirmed: the viscosity rapidly decayed following a WLF dependence as the temperature initially increased above the T_g followed by a more gradual Arrhenius decay in viscosity at higher temperatures (Figure 10B).

Recently, our group leveraged vinylogous urethane exchange⁹¹ for a straightforward synthesis of vinylogous urethane-containing PMMA vitrimers from inexpensive and commercially available monomers and crosslinkers (Figure 10C).⁷¹ We pre-synthesized linear polymers of MMA and 2-(acetoacetoxy)ethyl methacrylate (AAEMA), a reactive β -ketoester-containing monomer, through controlled radical polymerization, enabling us to precisely tune the molecular weight and composition of network strands within the eventual vitrimer material. Poly(MMA-*co*-AAEMA) was crosslinked with the use of excess tris(2-aminoethyl)amine by solution casting followed by compression molding. These vitrimers retained their chemical and thermal properties over multiple reprocessing cycles, and the mechanical properties were comparable with those of commodity PMMA counterparts. We also found that increasing the concentration of the moiety that promotes exchange (in our case free amino groups) within the network produced faster stress relaxation, which agrees well with other examples previously discussed.^{67,92}

The modification of non-exchangeable polymer backbones such as HDPE, PS, or PMMA certainly represents an attractive avenue for the generation of commodity bulk vitrimers. However, phase separation effects⁹³ must be taken into account if crosslinker and network strands are only moderately miscible. For example, PE modified with dioxaborolane moieties formed hierarchical nanostructures in which dioxaborolane-rich regions packed into a fractal-like arrangement.⁹⁴ Similar effects were also observed with DA-crosslinked ethylene–propylene rubber, where the heterogeneously cross-

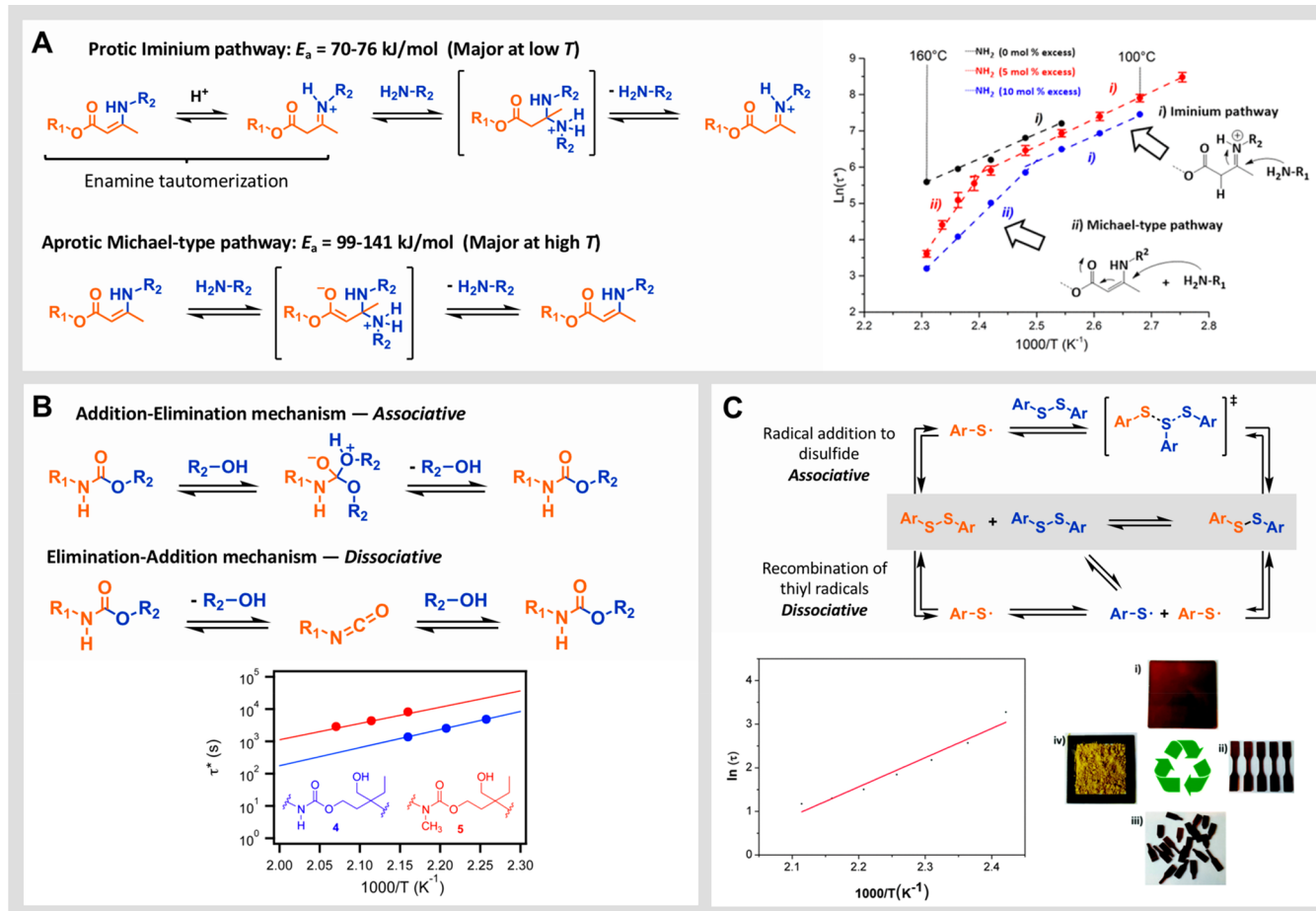


Figure 11. Illustration of covalent adaptable networks (CANs) with multiple bond exchange mechanisms. (A) Proposed mechanisms for vinyllogous urethane exchange at different temperatures. The change in mechanism, from the lower activation energy (E_a) protic iminium pathway to the higher E_a aprotic Michael-type pathway at elevated temperatures, was observed by a dramatic E_a change observed in Arrhenius plot. Reproduced with permission from ref 92. Copyright 2018 American Chemical Society. (B) Urethane exchange can occur via associative addition–elimination with free hydroxyl groups or via a Lewis acid-catalyzed dissociative elimination-addition reaction (top). The Arrhenius plot of methylated and non-methylated urethane networks shows similar activation energies of 101 ± 7 and $111 \pm 10 \text{ kJ/mol}$, respectively. Reproduced with permission from ref 90. Copyright 2015 American Chemical Society. (C) Radical-mediated aromatic disulfide exchange can proceed via associative radical addition or a dissociative radical recombination (top). The Arrhenius plot for the disulfide network shows a slight curvature, potentially due to increased disulfide cleavage at higher temperatures (left). Representative images of disulfide epoxy networks after reprocessing (right). Reproduced with permission from ref 98. Copyright 2016 Royal Society of Chemistry.

linked rubber exhibited an enhanced Young's modulus.⁹⁵ Rather than being viewed as a detrimental effect, however, perhaps immiscibility effects can be harnessed as a means to tune the mechanical and rheological properties of CANs in general, regardless of the crosslinking chemistry.

4. CANs WITH MIXED MECHANISMS OF BOND EXCHANGE

During our description of associative CANs, we discussed the concept and advantages of modifying viscoelastic properties through the use of chemical additives (e.g., catalysts, bases, modified crosslinkers, etc.). This strategy involves changing the mechanism—and consequently E_a —of dynamic bond exchange, which in turn influences the temperature-dependent material properties. Yet, an exogenous reagent is not always required. In some vitrimer systems, the mechanism of bond exchange is proposed to inherently change as a function of temperature. In an illustrative example by Du Prez and co-workers, fluorinated vinyllogous urethane vitrimers were synthesized by the crosslinking of perfluoropolyethers bearing

chain-end β -ketoester moieties with trifunctional amines to target elastomers with 0, 5, and 10 mol% excess primary amines.⁹² Interestingly, the networks containing 5 and 10 mol % excess amines were observed to have a dual temperature response as shown in the Arrhenius relationship, with a change in E_a for viscous flow from $70\text{--}76 \text{ kJ mol}^{-1}$ at lower temperatures to $99\text{--}141 \text{ kJ mol}^{-1}$ at higher temperatures (Figure 11A). It was hypothesized that this response is due to a change in mechanism, from a lower energy pathway involving transamination via an activated iminium intermediate to a higher energy pathway involving transamination via the more commonly cited conjugate addition reaction to the enaminone. This dual behavior has not been observed in other vinyllogous urethane vitrimer systems, suggesting that the network structure of these vitrimers may facilitate one mechanism over another. In view of this result, we again argue that the behavior of vitrimers should not be simplified to merely the exchange reaction of the dynamic crosslinks; instead, it is the confluence of the exchange mechanism, network topology, and

physical/thermal behavior of the network strands, among other factors, that begets the material's properties.

Urethane exchange with hydroxyl groups is another commonly employed reaction for the generation of thermally activated CANs,⁹⁶ and it is also one that can be imagined to proceed by either an associative or dissociative mechanism. When excess free alcohol is present, associative exchange could occur via an addition–elimination mechanism, while dissociative exchange would involve initial β -elimination to release an alcohol and an isocyanate (Figure 11B). Dichtel and co-workers devised a clever strategy to distinguish the two mechanisms, in which polyurethane networks bearing either *N*-methyl or *N*-hydrogen substituents were prepared and characterized.⁹⁰ In the hydrogen-bearing derivative, either an associative or dissociative mechanism would be feasible, whereas the methylated derivative is unable to undergo dissociation into a neutral isocyanate and alcohol; therefore, bond exchange is possible only by an associative mechanism. A comparison of the stress relaxation behavior revealed similar activation energies of viscous flow; therefore, it was deduced that associative transcarbamoylation of the *N*-hydrogen network was likely operative in the presence of a stoichiometric amount of hydroxy groups.⁸ However, in a later study it was found that urethane dissociation catalyzed by Lewis acids results in fast bond exchange in networks without an excess of hydroxyl groups.⁹⁷

One final example of potentially hybrid crosslink exchange that we wish to describe is the metathesis of aryl disulfides. As an example of the utility of this chemistry, Odriozola and co-workers synthesized disulfide-crosslinked epoxy vitrimers employing the rapid exchange of aryl disulfides.⁹⁸ Within the probed temperature range, the disulfide-epoxy material exhibited viscoelastic properties typical for vitrimers (Figure 11C). However, radical-mediated disulfide exchange could occur via associative disulfide exchange (in which a thiyl radical derived from a cleaved disulfide undergoes addition to a different disulfide) or dissociative disulfide cleavage followed by recombination. Recent work by Asua and co-workers illustrated the potential for both of these mechanisms to be active through small-molecule studies.⁹⁹ Moreover, it was shown that reductants such as tertiary amines could reduce the intermediate thiyl radical quickly to thiolates, which can then undergo thiolate–disulfide exchange. This potential pathway is particularly important for epoxy systems where tertiary amines are used as polymerization catalysts.

5. CONCLUSIONS AND OUTLOOK

Throughout this Perspective, we have primarily explored the fundamental properties of CANs while illustrating the diversity of reactions that can give rise to crosslink reversibility. Yet while the study of CANs has matured remarkably in less than two decades, there still remain several theoretical, experimental, and practical challenges that should be resolved before these materials can be applied in more ambitious directions. We will specifically emphasize the need for thorough and unambiguous material characterization, methods to supplement crosslink exchange in CANs for enhanced properties, and finally incorporation of CANs in industrially useful materials.

On several occasions in the previous sections, we noted that both dissociative CANs and vitrimers can exhibit Arrhenius stress relaxation, particularly under conditions where dissociative CANs retain a high degree of crosslink association. Yet, Arrhenius stress relaxation is sometimes used as sole

evidence of associative bond exchange, though it is by no means exclusive to vitrimers. More thorough characterization of crosslink exchange should therefore be provided if it is desired to specify an associative or dissociative mechanism. In the event that determining the bond exchange kinetics in the networks themselves is challenging, small molecule model reactions and, if spectroscopic methods reach their limits, simulations of the reaction pathway should be employed. We additionally wish to point out that even in the absence of corroborating an exchange mechanism, caution should be taken when analyzing and interpreting stress relaxation data. If this data is used to determine the characteristic relaxation time of a network, it should be remembered that the relaxation of polymers and networks is usually comprised of a multitude of different relaxation modes^{68,100} and therefore should often be modeled by a stretched exponential^{101–103} rather than a single Maxwell element.

The dynamic crosslink is the key distinguishing feature of CANs and is responsible for many of their properties; however, the incorporation of orthogonal crosslinks, both dynamic and non-dynamic, can be cleverly leveraged to improve the mechanical properties of covalent adaptable materials without impeding their reprocessability. For example, the incorporation of secondary sacrificial dynamic crosslinks that can dissipate energy greatly enhances the toughness and tensile strength of the covalent adaptable material.¹⁰⁴ Hydrogen bond-containing crosslinks in particular are useful due their dissociation at high temperatures, which improves network strand mobility and enhances flow during reprocessing.¹⁰⁵ On the other end of the spectrum, as we have shown in organoboron-containing materials,¹⁰⁶ permanent crosslinks can be incorporated to improve dimensional stability (i.e., creep resistance) at service temperatures while still allowing reprocessability at elevated temperatures. As elegantly described by Torkelson and co-workers, partially permanently crosslinked thermoreversible networks with maximum creep resistance can be generated by limiting the fraction of permanent crosslinks to a degree where no percolating permanent network is formed.¹⁰⁰ This critical degree of permanent crosslinking can be conveniently determined via modified Flory–Stockmayer theory. However, the incorporation of permanent crosslinks ultimately limits the complete chemical recycling of the material. Perhaps, replacing the permanent crosslinker with an orthogonal stimulus-responsive crosslinker that reverts upon a stimulus other than heat could be a solution to this drawback. A promising approach to modulating bond exchange and potentially enhancing dimensional stability is the use of photoresponsive thermoreversible DA crosslinkers. For example, a diarylethene photoswitch conjugated with the DA linkage can undergo a 6π electrocyclization upon UV irradiation and suppress the thermoreversibility of the DA crosslink.¹⁰⁷ Although visible light will eventually induce retro-electrocyclization and restore the thermoreversibility of the DA photoswitch linkages, which could impede the long-term stability of these materials, the concept of switchable bond exchange bears great potential for future applications in CANs.

With a plethora of exchange chemistries and polymer backbone types available for the generation of thermoreversible CANs, future research should further promote the translation of these materials from the laboratory to industrially relevant procedures in terms of production and processing. One approach is the incorporation of CANs into high-performance materials, such as covalent adaptable network composites that

contain CANs reinforced with fillers such as carbon fibers^{98,108} or silica particles.¹⁰⁹ Like in conventional polymer composites, the interactions between filler and the CAN matrix play a pivotal role in determining the material's mechanical properties. For example, fillers modified with functional groups that can participate in the dynamic bond exchange can accelerate stress relaxation; however, the covalent interaction between network and filler can result in a loss of crosslink density after reprocessing.¹⁰⁹

Equally important to translating CANs to industrially relevant materials is developing methodologies that are compatible with commercial synthetic techniques. Inspiring results have been achieved generating transesterification vitrimers via solid-state polymerization,¹¹⁰ reactive extrusion,¹¹¹ additive manufacturing,^{112,113} or emulsion polymerization.¹¹⁴ Another enticing example where CANs outperform commercial plastics is the generation of crosslinked melt-blown fibers.¹¹⁵ Melt-blowing of DA-based CANs provided cross-linked non-woven fiber sheets in one step, while conventional crosslinking techniques are not amenable to melt-blowing and require additional post-fabrication curing steps to generate those materials. Ultimately, the successful commercialization of a covalent adaptable material will require significant cost optimization and scalability at all stages, including chemical feedstocks, synthetic protocols, and processing. We are optimistic about the future prospects of CANs and believe they hold great promise in terms of outperforming current commodity materials. We therefore urge researchers in the area to continuously seek to expand the toolbox of fundamental CAN techniques while also considering means by which existing approaches can be made more translational.

AUTHOR INFORMATION

Corresponding Author

*sumerlin@chem.ufl.edu

ORCID

Jacob J. Lessard: [0000-0003-2962-6472](https://orcid.org/0000-0003-2962-6472)

Brent S. Sumerlin: [0000-0001-5749-5444](https://orcid.org/0000-0001-5749-5444)

Author Contributions

[‡]G.M.S. and J.J.L. contributed equally.

Notes

The authors declare no competing financial interest.

ACKNOWLEDGMENTS

This material is based upon work supported by the National Science Foundation (DMR-1904631).

REFERENCES

- (1) Staudinger, H. Über Polymerisation. *Ber. Dtsch. Chem. Ges. A/B* **1920**, *53*, 1073–1085.
- (2) Peters, E. N. Engineering Thermoplastics—Materials, Properties, Trends. In *Applied Plastics Engineering Handbook*, 2nd ed.; Kutz, M., Ed.; William Andrew Publishing: 2017; pp 3–26.
- (3) Pascault, J. P.; Williams, R. J. J. Overview of thermosets: Present and future. In *Thermosets*, 2nd ed.; Guo, Q., Ed.; Elsevier: 2018; pp 3–34.
- (4) Garcia, J. M.; Robertson, M. L. The future of plastics recycling. *Science* **2017**, *358*, 870–872.
- (5) Morales Ibarra, R. Recycling of thermosets and their composites. In *Thermosets*, 2nd ed.; Guo, Q., Ed.; Elsevier: 2018; pp 639–666.
- (6) Zhu, Y.; Romain, C.; Williams, C. K. Sustainable polymers from renewable resources. *Nature* **2016**, *540*, 354–362.
- (7) Sumerlin, B. S. Next-generation self-healing materials. *Science* **2018**, *362*, 150–151.
- (8) Fortman, D. J.; Brutman, J. P.; De Hoe, G. X.; Snyder, R. L.; Dichtel, W. R.; Hillmyer, M. A. Approaches to Sustainable and Continually Recyclable Cross-Linked Polymers. *ACS Sustainable Chem. Eng.* **2018**, *6*, 11145–11159.
- (9) Wojtecki, R. J.; Meador, M. A.; Rowan, S. J. Using the dynamic bond to access macroscopically responsive structurally dynamic polymers. *Nat. Mater.* **2011**, *10*, 14–27.
- (10) Bowman, C. N.; Kloxin, C. J. Covalent Adaptable Networks: Reversible Bond Structures Incorporated in Polymer Networks. *Angew. Chem., Int. Ed.* **2012**, *51*, 4272–4274.
- (11) Heinzmann, C.; Weder, C.; de Espinosa, L. M. Supramolecular polymer adhesives: advanced materials inspired by nature. *Chem. Soc. Rev.* **2016**, *45*, 342–358.
- (12) Roy, N.; Bruchmann, B.; Lehn, J.-M. DYNAMERS: dynamic polymers as self-healing materials. *Chem. Soc. Rev.* **2015**, *44*, 3786–3807.
- (13) Whittell, G. R.; Hager, M. D.; Schubert, U. S.; Manners, I. Functional soft materials from metallopolymers and metallosupramolecular polymers. *Nat. Mater.* **2011**, *10*, 176–188.
- (14) Voorhaar, L.; Hoogenboom, R. Supramolecular polymer networks: hydrogels and bulk materials. *Chem. Soc. Rev.* **2016**, *45*, 4013–4031.
- (15) Rossow, T.; Seiffert, S. Supramolecular Polymer Networks: Preparation, Properties, and Potential. In *Supramolecular Polymer Networks and Gels*; Seiffert, S., Ed.; Springer: 2015; pp 1–46.
- (16) Chen, X.; Dam, M. A.; Ono, K.; Mal, A.; Shen, H.; Nutt, S. R.; Sheran, K.; Wudl, F. A Thermally Re-mendable Cross-Linked Polymeric Material. *Science* **2002**, *295*, 1698–1702.
- (17) Kloxin, C. J.; Bowman, C. N. Covalent adaptable networks: smart, reconfigurable and responsive network systems. *Chem. Soc. Rev.* **2013**, *42*, 7161–7173.
- (18) Denissen, W.; Winne, J. M.; Du Prez, F. E. Vitrimers: permanent organic networks with glass-like fluidity. *Chem. Sci.* **2016**, *7*, 30–38.
- (19) Montarnal, D.; Capelot, M.; Tournilhac, F.; Leibler, L. Silica-Like Malleable Materials from Permanent Organic Networks. *Science* **2011**, *334*, 965–968.
- (20) Oehlenschlaeger, K. K.; Mueller, J. O.; Brandt, J.; Hilf, S.; Lederer, A.; Wilhelm, M.; Graf, R.; Coote, M. L.; Schmidt, F. G.; Barner-Kowollik, C. Adaptable Hetero Diels–Alder Networks for Fast Self-Healing under Mild Conditions. *Adv. Mater.* **2014**, *26*, 3561–3566.
- (21) Reutenauer, P.; Buhler, E.; Boul, P. J.; Candau, S. J.; Lehn, J. M. Room Temperature Dynamic Polymers Based on Diels–Alder Chemistry. *Chem. - Eur. J.* **2009**, *15*, 1893–1900.
- (22) Bergman, S. D.; Wudl, F. Mendable polymers. *J. Mater. Chem.* **2008**, *18*, 41–62.
- (23) Adzima, B. J.; Aguirre, H. A.; Kloxin, C. J.; Scott, T. F.; Bowman, C. N. Rheological and Chemical Analysis of Reverse Gelation in a Covalently Cross-Linked Diels–Alder Polymer Network. *Macromolecules* **2008**, *41*, 9112–9117.
- (24) Billiet, S.; De Bruycker, K.; Driessens, F.; Goossens, H.; Van Speybroeck, V.; Winne, J. M.; Du Prez, F. E. Triazolinediones enable ultrafast and reversible click chemistry for the design of dynamic polymer systems. *Nat. Chem.* **2014**, *6*, 815.
- (25) Van Herck, N.; Du Prez, F. E. Fast Healing of Polyurethane Thermosets Using Reversible Triazolinedione Chemistry and Shape-Memory. *Macromolecules* **2018**, *51*, 3405–3414.
- (26) Ying, H.; Zhang, Y.; Cheng, J. Dynamic urea bond for the design of reversible and self-healing polymers. *Nat. Commun.* **2014**, *5*, 3218.
- (27) Zhang, Y.; Ying, H.; Hart, K. R.; Wu, Y.; Hsu, A. J.; Coppola, A. M.; Kim, T. A.; Yang, K.; Sottos, N. R.; White, S. R.; Cheng, J.

Malleable and Recyclable Poly(urea-urethane) Thermosets bearing Hindered Urea Bonds. *Adv. Mater.* **2016**, *28*, 7646–7651.

(29) Zhang, L.; Rowan, S. J. Effect of Sterics and Degree of Cross-Linking on the Mechanical Properties of Dynamic Poly(alkylurea-urethane) Networks. *Macromolecules* **2017**, *50*, 5051–5060.

(30) Liu, W.-X.; Zhang, C.; Zhang, H.; Zhao, N.; Yu, Z.-X.; Xu, J. Oxime-Based and Catalyst-Free Dynamic Covalent Polyurethanes. *J. Am. Chem. Soc.* **2017**, *139*, 8678–8684.

(31) Obadia, M. M.; Mudrabyina, B. P.; Serghei, A.; Montarnal, D.; Drockenmuller, E. Reprocessing and Recycling of Highly Cross-Linked Ion-Conducting Networks through Transalkylation Exchanges of C–N Bonds. *J. Am. Chem. Soc.* **2015**, *137*, 6078–6083.

(32) Obadia, M. M.; Jourdain, A.; Cassagnau, P.; Montarnal, D.; Drockenmuller, E. Tuning the Viscosity Profile of Ionic Vitrimers Incorporating 1,2,3-Triazolium Cross-Links. *Adv. Funct. Mater.* **2017**, *27*, 1703258.

(33) Chakma, P.; Digby, Z. A.; Shulman, M. P.; Kuhn, L. R.; Morley, C. N.; Sparks, J. L.; Konkolewicz, D. Anilinium Salts in Polymer Networks for Materials with Mechanical Stability and Mild Thermally Induced Dynamic Properties. *ACS Macro Lett.* **2019**, *8*, 95–100.

(34) Cash, J. J.; Kubo, T.; Bapat, A. P.; Sumerlin, B. S. Room-Temperature Self-Healing Polymers Based on Dynamic-Covalent Boronic Esters. *Macromolecules* **2015**, *48*, 2098–2106.

(35) Chao, A.; Zhang, D. Investigation of Secondary Amine-Derived Aminal Bond Exchange toward the Development of Covalent Adaptable Networks. *Macromolecules* **2019**, *52*, 495–503.

(36) Zhang, B.; Digby, Z. A.; Flum, J. A.; Chakma, P.; Saul, J. M.; Sparks, J. L.; Konkolewicz, D. Dynamic Thiol–Michael Chemistry for Thermoresponsive Rehealable and Malleable Networks. *Macromolecules* **2016**, *49*, 6871–6878.

(37) Baruah, R.; Kumar, A.; Ujjwal, R. R.; Kedia, S.; Ranjan, A.; Ojha, U. Recyclable Thermosets Based on Dynamic Amidation and Aza-Michael Addition Chemistry. *Macromolecules* **2016**, *49*, 7814–7824.

(38) Griebel, J. J.; Nguyen, N. A.; Astashkin, A. V.; Glass, R. S.; Mackay, M. E.; Char, K.; Pyun, J. Preparation of Dynamic Covalent Polymers via Inverse Vulcanization of Elemental Sulfur. *ACS Macro Lett.* **2014**, *3*, 1258–1261.

(39) Kleine, T. S.; Nguyen, N. A.; Anderson, L. E.; Namnabat, S.; LaVilla, E. A.; Showghi, S. A.; Dirlam, P. T.; Arrington, C. B.; Manchester, M. S.; Schwiegerling, J.; Glass, R. S.; Char, K.; Norwood, R. A.; Mackay, M. E.; Pyun, J. High Refractive Index Copolymers with Improved Thermomechanical Properties via the Inverse Vulcanization of Sulfur and 1,3,5-Triisopropenylbenzene. *ACS Macro Lett.* **2016**, *5*, 1152–1156.

(40) Liu, H.; Nelson, A. Z.; Ren, Y.; Yang, K.; Ewoldt, R. H.; Moore, J. S. Dynamic Remodeling of Covalent Networks via Ring-Opening Metathesis Polymerization. *ACS Macro Lett.* **2018**, *7*, 933–937.

(41) Amamoto, Y.; Kikuchi, M.; Masunaga, H.; Sasaki, S.; Otsuka, H.; Takahara, A. Reorganizable Chemical Polymer Gels Based on Dynamic Covalent Exchange and Controlled Monomer Insertion. *Macromolecules* **2009**, *42*, 8733–8738.

(42) Jin, K.; Li, L.; Torkelson, J. M. Recyclable Crosslinked Polymer Networks via One-Step Controlled Radical Polymerization. *Adv. Mater.* **2016**, *28*, 6746–6750.

(43) Takahashi, A.; Goseki, R.; Ito, K.; Otsuka, H. Thermally Healable and Reprocessable Bis(hindered amino)disulfide-Cross-Linked Polymethacrylate Networks. *ACS Macro Lett.* **2017**, *6*, 1280–1284.

(44) Takahashi, A.; Goseki, R.; Otsuka, H. Thermally Adjustable Dynamic Disulfide Linkages Mediated by Highly Air-Stable 2,2,6,6-Tetramethylpiperidine-1-sulfanyl (TEMPS) Radicals. *Angew. Chem., Int. Ed.* **2017**, *56*, 2016–2021.

(45) Zhang, Z. P.; Rong, M. Z.; Zhang, M. Q. Mechanically Robust, Self-Healable, and Highly Stretchable “Living” Crosslinked Polyurethane Based on a Reversible C–C Bond. *Adv. Funct. Mater.* **2018**, *28*, 1706050.

(46) Zhang, C.; Liu, Z.; Shi, Z.; Yin, J.; Tian, M. Versatile Approach to Building Dynamic Covalent Polymer Networks by Stimulating the Dormant Groups. *ACS Macro Lett.* **2018**, *7*, 1371–1375.

(47) Amamoto, Y.; Kamada, J.; Otsuka, H.; Takahara, A.; Matyjaszewski, K. Repeatable photoinduced self-healing of covalently crosslinked polymers through reshuffling of trithiocarbonate units. *Angew. Chem., Int. Ed.* **2011**, *50*, 1660–1663.

(48) Michal, B. T.; Jaye, C. A.; Spencer, E. J.; Rowan, S. J. Inherently Photohealable and Thermal Shape-Memory Polydisulfide Networks. *ACS Macro Lett.* **2013**, *2*, 694–699.

(49) Hu, W.; Ren, Z.; Li, J.; Askounis, E.; Xie, Z.; Pei, Q. New Dielectric Elastomers with Variable Moduli. *Adv. Funct. Mater.* **2015**, *25*, 4827–4836.

(50) Zhang, G.; Zhao, Q.; Yang, L.; Zou, W.; Xi, X.; Xie, T. Exploring Dynamic Equilibrium of Diels–Alder Reaction for Solid State Plasticity in Remoldable Shape Memory Polymer Network. *ACS Macro Lett.* **2016**, *5*, 805–808.

(51) Schneiderman, D. K.; Hillmyer, M. A. 50th Anniversary Perspective: There Is a Great Future in Sustainable Polymers. *Macromolecules* **2017**, *50*, 3733–3749.

(52) Zhang, Y.; Broekhuis, A. A.; Picchioni, F. Thermally Self-Healing Polymeric Materials: The Next Step to Recycling Thermoset Polymers? *Macromolecules* **2009**, *42*, 1906–1912.

(53) Polgar, L. M.; van Duin, M.; Broekhuis, A. A.; Picchioni, F. Use of Diels–Alder Chemistry for Thermoreversible Cross-Linking of Rubbers: The Next Step toward Recycling of Rubber Products? *Macromolecules* **2015**, *48*, 7096–7105.

(54) Flory, P. J. Molecular Size Distribution in Three Dimensional Polymers. I. Gelation¹. *J. Am. Chem. Soc.* **1941**, *63*, 3083–3090.

(55) Stockmayer, W. H. Theory of Molecular Size Distribution and Gel Formation in Branched-Chain Polymers. *J. Chem. Phys.* **1943**, *11*, 45–55.

(56) Rubinstein, M.; Semenov, A. N. Thermoreversible Gelation in Solutions of Associating Polymers. 2. Linear Dynamics. *Macromolecules* **1998**, *31*, 1386–1397.

(57) Sheridan, R. J.; Adzima, B. J.; Bowman, C. N. Temperature Dependent Stress Relaxation in a Model Diels–Alder Network. *Aust. J. Chem.* **2011**, *64*, 1094–1099.

(58) Sheridan, R. J.; Bowman, C. N. A Simple Relationship Relating Linear Viscoelastic Properties and Chemical Structure in a Model Diels–Alder Polymer Network. *Macromolecules* **2012**, *45*, 7634–7641.

(59) Kuang, X.; Liu, G.; Dong, X.; Wang, D. Correlation between stress relaxation dynamics and thermochemistry for covalent adaptive networks polymers. *Mater. Chem. Front.* **2017**, *1*, 111–118.

(60) Chen, Q.; Huang, C.; Weiss, R. A.; Colby, R. H. Viscoelasticity of Reversible Gelation for Ionomers. *Macromolecules* **2015**, *48*, 1221–1230.

(61) Rubinstein, M.; Semenov, A. N. Dynamics of Entangled Solutions of Associating Polymers. *Macromolecules* **2001**, *34*, 1058–1068.

(62) Pratchayanan, D.; Yang, J.-C.; Lewis, C. L.; Thoppey, N.; Anthamatten, M. Thermomechanical insight into the reconfiguration of Diels–Alder networks. *J. Rheol.* **2017**, *61*, 1359–1367.

(63) Liu, Z.; Yu, C.; Zhang, C.; Shi, Z.; Yin, J. Revisiting Acetoacetyl Chemistry to Build Malleable Cross-Linked Polymer Networks via Transamidation. *ACS Macro Lett.* **2019**, *8*, 233–238.

(64) Ngai, K. L.; Plazek, D. J. Relation of internal rotational isomerism barriers to the flow activation energy of entangled polymer melts in the high-temperature Arrhenius region. *J. Polym. Sci., Polym. Phys. Ed.* **1985**, *23*, 2159–2180.

(65) Liu, C.-Y.; He, J.; Keunings, R.; Bailly, C. New Linearized Relation for the Universal Viscosity–Temperature Behavior of Polymer Melts. *Macromolecules* **2006**, *39*, 8867–8869.

(66) Capelot, M.; Montarnal, D.; Tournilhac, F.; Leibler, L. Metal-Catalyzed Transesterification for Healing and Assembling of Thermosets. *J. Am. Chem. Soc.* **2012**, *134*, 7664–7667.

(67) Snyder, R. L.; Fortman, D. J.; De Hoe, G. X.; Hillmyer, M. A.; Dichtel, W. R. Reprocessable Acid-Degradable Polycarbonate Vitrimers. *Macromolecules* **2018**, *51*, 389–397.

(68) Self, J. L.; Dolinski, N. D.; Zayas, M. S.; Read de Alaniz, J.; Bates, C. M. Brønsted-Acid-Catalyzed Exchange in Polyester Dynamic Covalent Networks. *ACS Macro Lett.* **2018**, *7*, 817–821.

(69) Denissen, W.; Rivero, G.; Nicolaÿ, R.; Leibler, L.; Winne, J. M.; Du Prez, F. E. Vinylogous Urethane Vitrimers. *Adv. Funct. Mater.* **2015**, *25*, 2451–2457.

(70) Denissen, W.; Droebeke, M.; Nicolaÿ, R.; Leibler, L.; Winne, J. M.; Du Prez, F. E. Chemical control of the viscoelastic properties of vinylogous urethane vitrimers. *Nat. Commun.* **2017**, *8*, 14857.

(71) Lessard, J. J.; Garcia, L. F.; Easterling, C. P.; Sims, M. B.; Bentz, K. C.; Arencibia, S.; Savin, D. A.; Sumerlin, B. S. Catalyst-Free Vitrimers from Vinyl Polymers. *Macromolecules* **2019**, *52*, 2105–2111.

(72) Ishibashi, J. S. A.; Kalow, J. A. Vitrimeric Silicone Elastomers Enabled by Dynamic Meldrum's Acid-Derived Cross-Links. *ACS Macro Lett.* **2018**, *7*, 482–486.

(73) Hendriks, B.; Waelkens, J.; Winne, J. M.; Du Prez, F. E. Poly(thioether) Vitrimers via Transalkylation of Trialkylsulfonium Salts. *ACS Macro Lett.* **2017**, *6*, 930–934.

(74) Zheng, P.; McCarthy, T. J. A surprise from 1954: siloxane equilibration is a simple, robust, and obvious polymer self-healing mechanism. *J. Am. Chem. Soc.* **2012**, *134*, 2024–7.

(75) Nishimura, Y.; Chung, J.; Muradyan, H.; Guan, Z. Silyl Ether as a Robust and Thermally Stable Dynamic Covalent Motif for Malleable Polymer Design. *J. Am. Chem. Soc.* **2017**, *139*, 14881–14884.

(76) Christensen, P. R.; Scheuermann, A. M.; Loeffler, K. E.; Helms, B. A. Closed-loop recycling of plastics enabled by dynamic covalent diketoneamine bonds. *Nat. Chem.* **2019**, *11*, 442–448.

(77) Lu, Y.-X.; Guan, Z. Olefin Metathesis for Effective Polymer Healing via Dynamic Exchange of Strong Carbon–Carbon Double Bonds. *J. Am. Chem. Soc.* **2012**, *134*, 14226–14231.

(78) Röttger, M.; Domenech, T.; van der Weegen, R.; Breuillac, A.; Nicolaÿ, R.; Leibler, L. High-performance vitrimers from commodity thermoplastics through dioxaborolane metathesis. *Science* **2017**, *356*, 62–65.

(79) Kotliar, A. M. Interchange reactions involving condensation polymers. *Macromol. Revs.* **1981**, *16*, 367–395.

(80) Porter, R. S.; Jonza, J. M.; Kimura, M.; Desper, C. R.; George, E. R. Polyesters II: A review of phase behavior in binary blends: Amorphous, crystalline, liquid crystalline, and on transreaction. *Polym. Eng. Sci.* **1989**, *29*, 55–62.

(81) Demongeot, A.; Mougnier, S. J.; Okada, S.; Soulie-Ziakovic, C.; Tournilhac, F. Coordination and catalysis of Zn^{2+} in epoxy-based vitrimers. *Polym. Chem.* **2016**, *7*, 4486–4493.

(82) Capelot, M.; Unterlass, M. M.; Tournilhac, F.; Leibler, L. Catalytic Control of the Vitrimer Glass Transition. *ACS Macro Lett.* **2012**, *1*, 789–792.

(83) Zhou, Y.; Groote, R.; Goossens, J. G. P.; Sijbesma, R. P.; Heuts, J. P. A. Tuning PBT vitrimer properties by controlling the dynamics of the adaptable network. *Polym. Chem.* **2019**, *10*, 136–144.

(84) Brutman, J. P.; Delgado, P. A.; Hillmyer, M. A. Polylactide Vitrimers. *ACS Macro Lett.* **2014**, *3*, 607–610.

(85) Liu, W.; Schmidt, D. F.; Reynaud, E. Catalyst Selection, Creep, and Stress Relaxation in High-Performance Epoxy Vitrimers. *Ind. Eng. Chem. Res.* **2017**, *56*, 2667–2672.

(86) Diehl, K. L.; Kolesnichenko, I. V.; Robotham, S. A.; Bachman, J. L.; Zhong, Y.; Brodbelt, J. S.; Anslyn, E. V. Click and chemically triggered declick reactions through reversible amine and thiol coupling via a conjugate acceptor. *Nat. Chem.* **2016**, *8*, 968–973.

(87) Denissen, W.; De Baere, I.; Van Paepegem, W.; Leibler, L.; Winne, J.; Du Prez, F. E. Vinylogous Urea Vitrimers and Their Application in Fiber Reinforced Composites. *Macromolecules* **2018**, *51*, 2054–2064.

(88) Lai, J. C.; Mei, J. F.; Jia, X. Y.; Li, C. H.; You, X. Z.; Bao, Z. A Stiff and Healable Polymer Based on Dynamic-Covalent Boroxine Bonds. *Adv. Mater.* **2016**, *28*, 8277–8282.

(89) Ogden, W. A.; Guan, Z. Recyclable, Strong, and Highly Malleable Thermosets Based on Boroxine Networks. *J. Am. Chem. Soc.* **2018**, *140*, 6217–6220.

(90) Fortman, D. J.; Brutman, J. P.; Cramer, C. J.; Hillmyer, M. A.; Dichtel, W. R. Mechanically Activated, Catalyst-Free Polyhydroxyurethane Vitrimers. *J. Am. Chem. Soc.* **2015**, *137*, 14019–14022.

(91) Sims, M. B.; Lessard, J. J.; Bai, L.; Sumerlin, B. S. Functional Diversification of Polymethacrylates by Dynamic β -Ketoester Modification. *Macromolecules* **2018**, *51*, 6380–6386.

(92) Guerre, M.; Tapani, C.; Nicolaÿ, R.; Winne, J. M.; Du Prez, F. E. Fluorinated Vitrimer Elastomers with a Dual Temperature Response. *J. Am. Chem. Soc.* **2018**, *140*, 13272–13284.

(93) Chen, X.; Li, L.; Wei, T.; Torkelson, J. M. Reprocessable Polymer Networks Designed with Hydroxyurethane Dynamic Cross-links: Effect of Backbone Structure on Network Morphology, Phase Segregation, and Property Recovery. *Macromol. Chem. Phys.* **2019**, *220*, 1900083.

(94) Ricarte, R. G.; Tournilhac, F.; Leibler, L. Phase Separation and Self-Assembly in Vitrimers: Hierarchical Morphology of Molten and Semicrystalline Polyethylene/Dioxaborolane Maleimide Systems. *Macromolecules* **2019**, *52*, 432–443.

(95) Polgar, L. M.; Hagting, E.; Raffa, P.; Mauri, M.; Simonutti, R.; Picchioni, F.; van Duin, M. Effect of Rubber Polarity on Cluster Formation in Rubbers Cross-Linked with Diels-Alder Chemistry. *Macromolecules* **2017**, *50*, 8955–8964.

(96) Brutman, J. P.; Delgado, P. A.; Hillmyer, M. A. Polylactide Vitrimers. *ACS Macro Lett.* **2014**, *3*, 607–610.

(97) Brutman, J. P.; Fortman, D. J.; De Hoe, G. X.; Dichtel, W. R.; Hillmyer, M. A. Mechanistic Study of Stress Relaxation in Urethane-Containing Polymer Networks. *J. Phys. Chem. B* **2019**, *123*, 1432–1441.

(98) Ruiz de Luzuriaga, A.; Martin, R.; Markaide, N.; Rekondo, A.; Cabañero, G.; Rodríguez, J.; Odriozola, I. Epoxy resin with exchangeable disulfide crosslinks to obtain reprocessable, repairable and recyclable fiber-reinforced thermoset composites. *Mater. Horiz.* **2016**, *3*, 241–247.

(99) Nevejans, S.; Ballard, N.; Miranda, J. I.; Reck, B.; Asua, J. M. The underlying mechanisms for self-healing of poly(disulfide)s. *Phys. Chem. Chem. Phys.* **2016**, *18*, 27577–27583.

(100) Li, L. Q.; Chen, X.; Jin, K. L.; Torkelson, J. M. Vitrimers Designed Both To Strongly Suppress Creep and To Recover Original Cross-Link Density after Reprocessing: Quantitative Theory and Experiments. *Macromolecules* **2018**, *51*, 5537–5546.

(101) Edholm, O.; Blomberg, C. Stretched exponentials and barrier distributions. *Chem. Phys.* **2000**, *252*, 221–225.

(102) Palmer, R. G.; Stein, D. L.; Abrahams, E.; Anderson, P. W. Models of Hierarchically Constrained Dynamics for Glassy Relaxation. *Phys. Rev. Lett.* **1984**, *53*, 958–961.

(103) Fancey, K. S. A mechanical model for creep, recovery and stress relaxation in polymeric materials. *J. Mater. Sci.* **2005**, *40*, 4827–4831.

(104) Neal, J. A.; Mozhdehi, D.; Guan, Z. Enhancing Mechanical Performance of a Covalent Self-Healing Material by Sacrificial Noncovalent Bonds. *J. Am. Chem. Soc.* **2015**, *137*, 4846–4850.

(105) Liu, Y.; Tang, Z.; Wu, S.; Guo, B. Integrating Sacrificial Bonds into Dynamic Covalent Networks toward Mechanically Robust and Malleable Elastomers. *ACS Macro Lett.* **2019**, *8*, 193–199.

(106) Cash, J. J.; Kubo, T.; Dobbins, D. J.; Sumerlin, B. S. Maximizing the symbiosis of static and dynamic bonds in self-healing boronic ester networks. *Polym. Chem.* **2018**, *9*, 2011–2020.

(107) Fuhrmann, A.; Gostl, R.; Wendt, R.; Kotteritzsch, J.; Hager, M. D.; Schubert, U. S.; Brademann-Jock, K.; Thunemann, A. F.; Nochel, U.; Behl, M.; Hecht, S. Conditional repair by locally switching the thermal healing capability of dynamic covalent polymers with light. *Nat. Commun.* **2016**, *7*, 13623.

(108) Taynton, P.; Ni, H.; Zhu, C.; Yu, K.; Loob, S.; Jin, Y.; Qi, H. J.; Zhang, W. Repairable Woven Carbon Fiber Composites with Full Recyclability Enabled by Malleable Polyimine Networks. *Adv. Mater.* **2016**, *28*, 2904–2909.

(109) Chen, X.; Li, L.; Wei, T.; Venerus, D. C.; Torkelson, J. M. Reprocessable Polyhydroxyurethane Network Composites: Effect of

Filler Surface Functionality on Cross-link Density Recovery and Stress Relaxation. *ACS Appl. Mater. Interfaces* **2019**, *11*, 2398–2407.

(110) Zhou, Y.; Goossens, J. G. P.; Sijbesma, R. P.; Heuts, J. P. A. Poly(butylene terephthalate)/Glycerol-based Vitrimers via Solid-State Polymerization. *Macromolecules* **2017**, *50*, 6742–6751.

(111) Demongeot, A.; Groote, R.; Goossens, H.; Hoeks, T.; Tournilhac, F.; Leibler, L. Cross-Linking of Poly(butylene terephthalate) by Reactive Extrusion Using Zn(II) Epoxy-Vitrimer Chemistry. *Macromolecules* **2017**, *50*, 6117–6127.

(112) Shi, Q.; Yu, K.; Kuang, X.; Mu, X.; Dunn, C. K.; Dunn, M. L.; Wang, T.; Jerry Qi, H. Recyclable 3D printing of vitrimer epoxy. *Mater. Horiz.* **2017**, *4*, 598–607.

(113) Zhang, B.; Kowsari, K.; Serjouei, A.; Dunn, M. L.; Ge, Q. Reprocessable thermosets for sustainable three-dimensional printing. *Nat. Commun.* **2018**, *9*, 1831.

(114) Tran, T. N.; Rawstron, E.; Bourgeat-Lami, E.; Montarnal, D. Formation of Cross-Linked Films from Immiscible Precursors through Sintering of Vitrimer Nanoparticles. *ACS Macro Lett.* **2018**, *7*, 376–380.

(115) Jin, K.; Kim, S.-s.; Xu, J.; Bates, F. S.; Ellison, C. J. Melt-Blown Cross-Linked Fibers from Thermally Reversible Diels–Alder Polymer Networks. *ACS Macro Lett.* **2018**, *7*, 1339–1345.